"On-Chip Reflector and Absorber based on High Index Contrast Grating on SOI Chip for Optoelectronic Devices"

Dissertation Submitted towards the partial fulfillment of requirement for the award of degree of

Master of Engineering

In

Electronics and Communication Engineering

Submitted by:

Sheenu Jindal

(801261021)

Under the guidance of:

Dr. Mukesh Kumar

ELECTRONICS AND COMMUNICATION ENGINEERING DEPARTMENT

THAPAR UNIVERSITY

(Established under the section 3 of UGC Act, 1956)

PATIALA – 147004 (PUNJAB)

DECLARATION

I **Sheenu Jindal**, hereby certify that the work which is presented in this dissertation entitled "On-Chip Reflector and Absorber based on High Index Contrast Grating on SOI Chip for Optoelectronic Devices" is an authentic record of my study carried out as requirement for the award of degree of ME (Electronics and Communication Engineering) at Thapar University, Patiala, under the supervision of **Dr. Mukesh Kumar.**

The matter presented in this dissertation has not been submitted in any other University/Institute for the award of any other degree.

Sheenu Jindal

Date: 14th July, 2014

Sheenu Jindal

(801261021)

It is certified that the above statement made by the student is correct to the best of my knowledge and belief.

Date: 14th July, 2014

Dr. Mukesh Kumar

Assistant Professor, ECED

Thapar University,Patiala

Countersigned By :

Dr.Sanjay Sharma

Professor and Head ECED

Thapar University,Patiala

Dr.S.K.Mohapatra

Dean of Academic Affairs

Thapar University,Patiala

ACKNOWLEDGEMENT

I would like to express my special thanks to my dissertation Advisor, **Dr. Mukesh Kumar,** Assistant Professor, Electronics & Communication Engineering Department, Thapar University, Patiala for his continuous indefatigable guidance and support. He has been an excellent advisor, as he is a great source not only of knowledge, experience and insight but also of inspiration and encouragement which paved me on to the path to carry this project. I am highly indebted to him for his painstaking efforts and invaluable suggestions during the period of work.

I am also thankful to Head of Department and Professor (**Dr.) Sanjay Sharma**, PG Coordinator **Dr. Kulbir Singh** (Associate Professor), and PG Co-Coordinator **Dr. Surbhi Sharma** (Assistant Professor) of Electronics & Communication Engineering Department, Thapar University, Patiala for their valuable advice and helped in all possible ways for the completion of my dissertation work.

My greatest thanks is to all who wished me success especially my parents. Above all I render my gratitude to the Almighty who bestowed self-confidence, ability and strength in me to complete this work, for not letting me down at the time of crisis and showing me the silver lining in the dark clouds. I do not find enough words with which I can express my feelings of thanks to my dear friends for their help, inspiration and moral support which went a long way in successful competition of the present study.

Sheenu jindal

(801261021)

ABSTRACT

In this dissertation, a novel single-layer subwavelength High-Index-Contrast Grating (HCG) is presented, which provides new and promising platform for integrated optoelectronics having applications in lasers, modulators, detectors. Broadband Reflector in near IR range using High Index Contrast Grating is proposed which provides large reflection (>98.5%) over a wavelength range of 1.31-1.76μm with large fabrication tolerance. HCG not only reduces the size of optical devices but also enhances their performance. Various applications of HCGs in optoelectronic devices, including vertical-cavity surface-emitting lasers (VCSELs), high-Q optical resonators, and hollow-core waveguides are discussed. HCG based narrowband Transmission filter is proposed at slightly off normal incidence angle (5˚) which is closer to surface normal incidence.

Also a simple design of a broadband terahertz absorber consisting of a High-index Contrast Grating (HCG) on a Silicon-on-insulator (SOI) chip is proposed. A large absorption (98.4%) over a frequency range of 3.57 - 4.54 THz is obtained with large fabrication tolerance (14μm period tolerance for grating height of 2.6μm). The absorption remains high (~ 98 %) for wide range of angle of incidence from 0˚ (Normal incidence) to 60˚. The bandwidth of high absorption (~ 98 %) is also large over a wide range of angles of incidence. The proposed broadband terahertz absorber also exhibits the design flexibility for the realization of polarization insensitivity with respect to the incident light with arbitrary polarizations. The proposed structure is easy-to-fabricate with a large fabrication tolerance which may provide a desirable broadband absorption for practical applications in terahertz devices. The proposed absorber is designed using Rigorous Coupled Wave Analysis (RCWA) and the results are in good agreement (with maximum difference of 0.6%) with those obtained with Finite difference time domain (FDTD) method. The proposed characteristics of the device arise from the broadband nature and wavelength scalability of the HCG.

TABLE OF CONTENTS

LIST OF FIGURES

LIST OF ACRONYMS

HCG	High Contrast Grating
DBR	Distributed Bragg Reflector
VCSEL	Vertical Cavity Surface Emitting Laser
FP	Fabry Perot
RCE	Resonant Cavity Enhanced
MA	Metamaterial Absorber
THz	Terahertz
RCWA	Rigorous Coupled Wave Analysis
FDTD	Finite difference Time Domain
DWDM	Dense Wavelength Division Multiplexing

Chapter

1 Optical Grating for Integrated Optoelectronics

1.1 Integrated Optoelectronics

Integrated Optoelectronics, in which devices such as detectors, lasers, and modulators are integrated with different electronic or optical devices on a single semiconductor chip, becomes key technology in flourishing future optical communication systems[1]. This is because of its essential benefits in realizing high-versatility, high-performance and high-functionality in optoelectronic devices, which have been developed partially due to the restricted use of conventional discrete devices and assembly techniques. A generalized optical system, to model the required performance of an optical system is shown in Figure1.1. Optoelectronic integrated transmitters and receivers[2] play an important role in light wave communication and interconnection applications. The monolithic integration of optical devices with electronic devices on a single semiconductor chip becomes the promising candidate for the realization of cheap and compact modules.

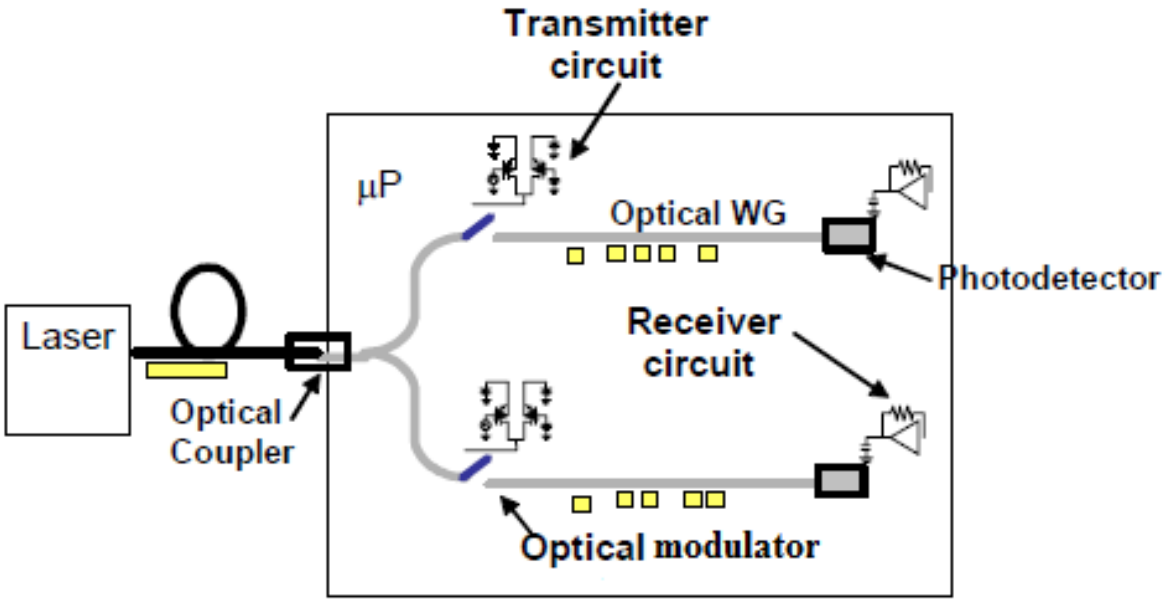

Figure 1.1 Model of Generalized Optical System [1].

Optoelectronic integration provides various optical processing functions on a single semiconductor chip and thus improves the properties of optoelectronic devices. Optical devices based on integrated light sources and also circuits based on waveguides for wavelength division multiplexing and optical heterodyne detection are its suitable examples. Optoelectronic integration is attractive not only for high data rate communication but also for computing and switching. Nowadays, Intra-chip communications [3] by means of integrated on-chip devices overcome the constraints of broadband signal transmissions between the inflexible integrated circuits. As the number of on-chip communicators increases, and as the programmers start utilizing the chips' parallel resources efficiently, the communication throughput increases to maintain global performance.

(a) Semiconductor Lasers

A laser is a device that emits light by the stimulated emission of electromagnetic radiation through the process of optical amplification. Lasers are unique from other optical sources due to their coherence[4]. Semiconductor lasers depends upon the gain media of the cavity, where gain is normally obtained by stimulated emission of radiation under the condition of population inversion (large carrier concentration in the conduction band as compared to the valence band at inter-band transition), which is achieved by the process called pumping. There are two main types of laser shown in Figure 1.2 Edge emitting laser with lateral optical feedback cavity and Surface emitting laser with longitudinal optical feedback cavity [5].

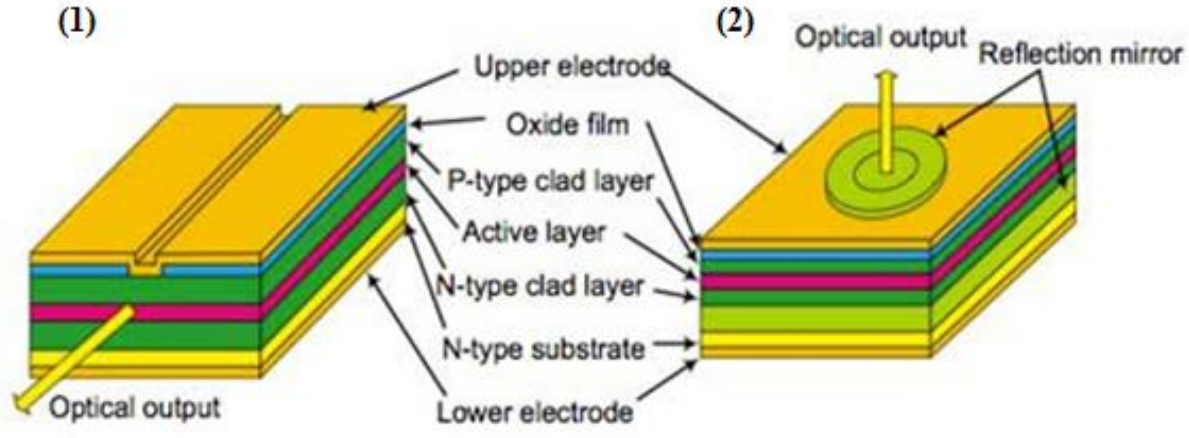

Figure 1.2 Two main types of laser (1) Transverse edge emitting laser structure (2) Vertical cavity surface emitting laser structure[5].

Due to large size of the cavity resonator in edge emitting lasers, the optical output is very high but provides multimode operation. Single mode oscillations are the major requirement in optical sources. So in order to obtain single mode operation in edge emitting lasers, Distributed Feedback(DFB) laser and Distributed Bragg Reflector (DBR) laser [6] structures in which gratings are integrated are utilized. In contrary, surface emitting lasers provide single mode operation and thus do not require any mode selection.

(b) Photodetector

Photodetectors are the devices that are used for the detection of light. The two possible designs of detectors are Resonant-cavity-enhanced (RCE) photodetectors[7, 8] and Fabry Perot (FP) photodetectors[9]. The structure of RCE photodetector is similar to other conventional photodetectors, but resonances in the optical cavity of RCE detectors enhances the optical field, and thus makes these photodetectors thinner and faster, and simultaneously increases the quantum efficiency at the resonant wavelengths. Figure 1.3 (a) shows the schematic drawing of the Resonant-cavity-enhanced photodetector that works on the principle that *p*-*i*-*n* detector having thin *i*-layer in the resonant cavity. The light is passed multiple times through this *i*-region to get absorbed and make this layer very thin in order to get fast output response. When the gap is moved, energy inside the cavity decreases and the mirror reflectance power changes, which further changes the cavity Q factor. The detector shows non-uniform response over wavelength tuning, even though it can be very efficient at some values of wavelengths [10].

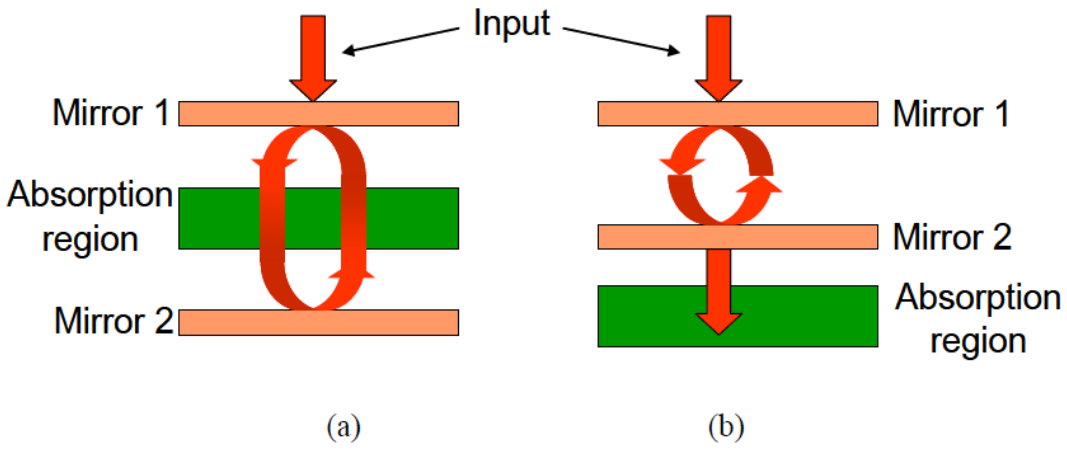

Figure 1.3 Schemetic drawing of two possible designs of photodetectors (a) Resonant Cavity photodetector (b) Fabry Perot Filter Detector [10].

Figure 1.3 (b) shows the schematic drawing of the Fabry-Perot (FP) tunable detector. The FP filter detector is less sensitive to cavity Quality factor, though it can also have the air gap as the cavity because responsivity depends on the matching between two mirrors and does not change significantly over wavelength tuning. Moreover, FP detector is easy to fabricate as filter and detector can be optimized independently due to its decomposition into two different devices.

(c) Optical modulators

Silicon optical modulators convert data in electrical domain to optical domain. It provides low-loss integration and cheap fiber packaging due to its high speed of operation and CMOS compatibility[11]. Modulators are used in intra-chip photonic communication. Ideally optical modulators are fast, reliable, scalable, low power and small in size. Typically, data capacity of electronic links can be enhanced by increasing the number of parallel wires in a bus. Alternatively, optical signal capacity can be enhanced by increasing the number of parallel wavelengths on a single waveguide. Therefore, the electro-optic translating device should convert between wavelength parallel photonics and space-parallel electronics in much simpler way. Micro-ring resonator based modulators comprising of a ring waveguide coupled to a single straight waveguide which provides space parallel electronic to wavelength parallel photonic translation is shown in Figure 1.4. Dashed outlines depict doping regions, solid lines shows photonic waveguides, and dotted lines represent electronic links.

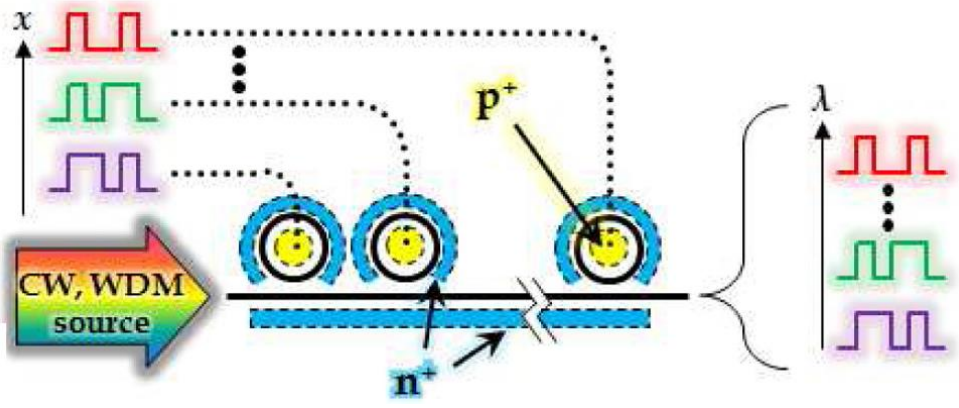

Figure 1.4 Schematic of space-parallel (x) electronic to wavelength-parallel (λ) photonic translation using micro-ring modulators[11].

Modulators based on thermo-optic effect [12] and free-carrier effect [13] suffers from many limitations. To avoid the limitation provided by these two structures, resonator based devices can be employed which provides high-speed modulation with low power consumption. The major advantage of ring modulator is that it modulates light at resonant wavelength of ring resonator and allows all other wavelengths to pass through it. As a result, the micro-ring resonator based modulators show attractive performances in terms of speed, size, and power consumption.

1.2 Role of grating in Optoelectronics

Gratings are always preferred when light of different wavelengths are to be separated with high resolution. It consists of large number of closely spaced parallel slits which provides very sharp and narrow intensity peak and provides very high resolution for numerous applications like spectroscopy, imaging, micro-chromators, wavelength division multiplexing devices. Such gratings can be either transmissive or reflective [14]. Figure 1.5 shows the binary blazed grating scheme for arrayed waveguide grating demodulation integration micro system. Gratings which modulates phase instead of amplitude of the light wave incident are produced with the help of holography[15].

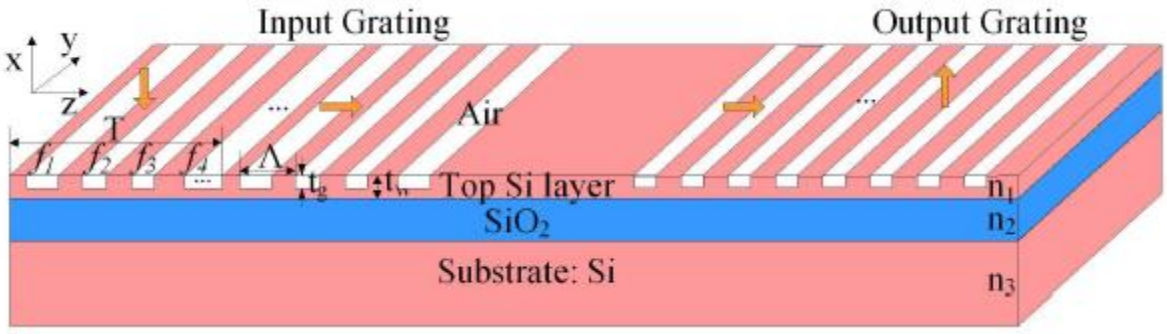

Figure1.5 Structure of the input and output gratings[16].

As the information industry is growing very rapidly throughout the world, the demands for the communication networks with high speed and larger capacity is also increasing. The optical fiber communication system plays an important role in modern communication networks. Normally, the transmission loss, dispersion, and the nonlinear effects are the main

obstacles faced by the optical fiber communication system. Transmission losses can be overcome by the use of the erbium doped fiber amplifier (EDFA) [16]; Nonlinear effects can also be suppressed by introducing some dispersion. Therefore, dispersion becomes the major difficulty in refining the optical fiber communication system. But with the advancement in optoelectronic devices, dispersion can also be compensated to provide high speed optical fiber transmission system. One such device is optical grating that plays a crucial role in the compensation of dispersion. By optimizing the fabrication process of Chirped Fiber Bragg Grating[17] many difficult problems i.e. the ripple of the time delay, loss due to cladding mode, fabrication repetition have been solved.

Gratings play an attractive role in Dense Wavelength Division Multiplexing (DWDM) optical networks. It increases the system performances in terms of selectivity and crosstalk between adjacent channels[18].

1.3 High Index Contrast Grating

1.3.1 Fundamentals

Optical grating has been extensively utilized in wide range of applications like holography, spectroscopy, lasers, modulators, detectors and many other optoelectronic devices. Optical gratings are the periodic structure comprising of a large number of equally spaced grooves. When light wave is incident onto the grating, it can be reflected or transmitted by these grooves. In Figure 1.6, a plane wave is incident at an angle θ_i with respect to the grating surface normal direction. For the light diffracted with an angle θ_d, the optical path difference between two adjacent grooves can be expressed as[19]

$$\Lambda \sin\theta_i - \Lambda \sin\theta_d \tag{1.1}$$

where Λ is the period of the grating. When this optical path difference equals to an integral multiple of the incident light wavelength, the light will interfere constructively in phase.

$$\Lambda \sin\theta_i - \Lambda \sin\theta_d = m\pi \tag{1.2}$$

$$\text{for } m = 0, \pm 1, \pm 2, \ldots$$

At some set of angles, the light scattered from grooves will be in phase and constructively interfere. At these angles, the reflectance of light is increased, while there would be destructive interference for all other angles[14]. The above analysis shows that gratings can

diffract incident light wave in a unique set of angles. This property of grating can be expressed as grating equation:

$$sin\theta_{d,m} - sin\theta_i = m\lambda/\Lambda \quad (1.3)$$

$$for\ m = 0,\pm1,\pm2,\ldots$$

where θ_i is the angle between the incident light and the grating surface normal direction, and $\theta_{d,m}$ is the angle between the *m-th* order diffraction light and the grating surface normal direction respectively. The integer *m* denotes diffraction order and λ is the operating wavelength. The above equations hold only for monochromatic and perfectly collimated light wave [19, 20].

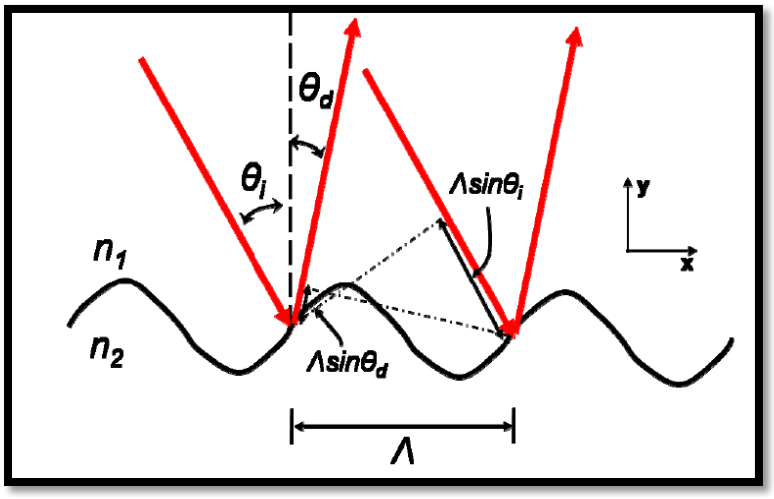

Figure 1.6 Schematic of an optical grating depicting the phase relationship among diffracted rays from the adjacent grooves[19].

Most diffraction gratings have grating period larger than the optical wavelength. However, when the period of grating becomes lesser than the operating wavelength, the grating will exhibit many exotic and unattainable properties[20]. A subwavelength grating is a grating having period lesser than the operating wavelength. If light is incident normally onto a subwavelength grating, only the 0^{th} order mode propagates and all other higher order modes are the evanescent modes. The grating will act as a simple reflective mirror.

Figure 1.7 shows the two gratings: one in which period is much larger than the wavelength (Diffraction Grating) and other in which period is less than the operating wavelength (High Contrast Grating).

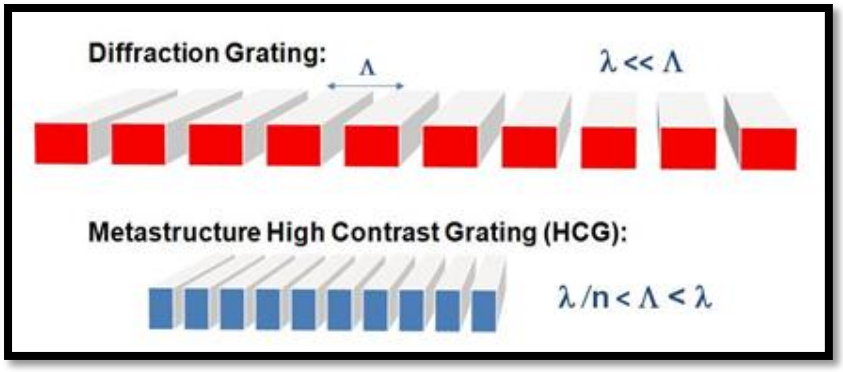

Figure 1.7 Diffraction Grating and HCG [20].

1.3.2 Applications of High index contrast Grating

(a) Polarization Insensitive Hollow Optical Waveguide

Attenuation and nonlinearities are faced when light interacts with the high refractive index material of the core in conventional dielectric waveguides, but this can be evaded when the light propagates in low index core having highly reflective walls[21]. A number of applications of hollow core optical waveguides are in sensing, optical communications, environmental applications, and spectroscopy. Temperature insensitivity and wide tuning range are two major characteristics of hollow waveguides (HWGs) [22] which can be utilized to create widely tunable photonic devices without the requirement of sensors that control temperature. At narrow air core, the HWGs are polarization dependent because it offers large tuning in propagation constant.

To reduce this dependence on polarization, the HCG mirror can be introduced which provides lateral periodicity in hollow waveguide [23]. Figure1.8 shows the design of polarization independent HWG. The overall polarization dependence of HWG is diminished by introducing a phase-matching layer in DBR and by optimizing the grating thickness of HCG mirror. The waveguide contains both vertical and lateral periodicity. It consists of a high index contrast grating acting as a top reflective mirror and DBR as bottom mirror of HWG. Light can be confined vertically in air-core due to the high reflectivities of DBR and HCG. A phase matching layer made of Si at the top of DBR is used to control the orthogonal polarizations[23]. The upper side of waveguide comprises of a high refractive index contrast (between air and silicon) grating. The net refractive index of the mode guided in the core

below the HCG is higher than that in the other two lateral parts of core where HCG is absent. The high index below HCG provides lateral optical confinement originating from a great phase change under HCG. The thickness of the high contrast grating and phase matching layer of DBR is optimized to alter the propagation characteristics of the orthogonal polarizations. These hollow waveguide are attractive for applications in polarization insensitive photonic devices [24] for photonic networks.

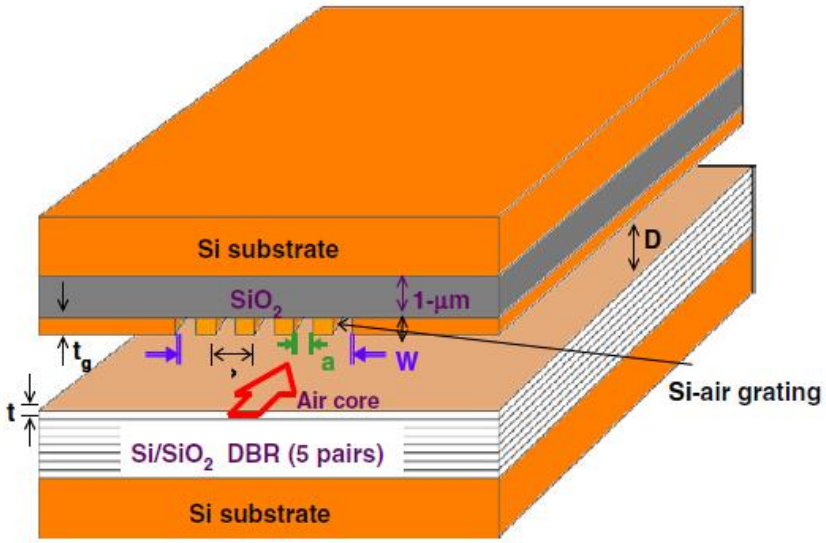

Figure1.8 Schematic of Hollow Optical Waveguide incorporating HCG as top mirror and DBR as bottom mirror with phase matching layer on top of DBR [21].

(b) Broadband Out-Coupler

Conventional Gratings offer small coupling strength therefore larger size gratings are to be used but they provides an out coupled beam which is much larger than the fiber mode. As a result, an additional lens is needed to couple to a fiber or, alternatively, a curved grating can be utilized that efficiently couples the light into a fiber. Due to large dimensions and low refractive index contrast, integrated optical devices allow a few functions to be incorporated on a chip. Nano-photonic circuits[25] on silicon-on-insulator (SOI) plays a crucial role in large-scale photonic integration because of the high refractive index contrast between Silicon and Silicon dioxide. The strong optical confinement is another characteristic of SOI photonic circuits. For many applications, there is a strong requirement of integrating electronic and

photonic devices on a single SOI chip. One of the challenges is to easily couple light into and out of SOI waveguides. Grating plays a great role in coupling light into an optical fiber when placed out of the plane of the waveguide, as it allows optical Inputs/outputs to populate any area of a planar light wave circuits instead of being restricted to just one edge of a chip. Optical gratings are the prime candidates to interact with on-chip optical components for coupling the light into the optical fibers or on/off chip devices for further optical processing [26]. High index contrast grating coupler maximizes the interaction of such gratings with the optical modes of the integrated optical devices. The schematic drawing of the out-coupler on SOI chip is shown in Figure 1.9 (a). The SOI waveguide comprises of silicon layer mounted on the top of the layer of silicon dioxide on a silicon substrate. A high-index contrast grating known as HCG is etched onto the top of the silicon layer. The thickness of SiO_2 has a major impact on the guiding characteristics of the grating [27]. The radiated wave coming downwards reflects partially at the dielectric-substrate interface. Figure 1.9 (b) shows the field propagation of light wave when incident from sideways in the *z* direction. The oxide thickness should be so chosen that the reflected wave interferes constructively with the directly upward radiated waves so as to enhance the coupling strength. The device can find applications in broadband high-Q resonator to effectively couple a wide band of wavelengths of light.

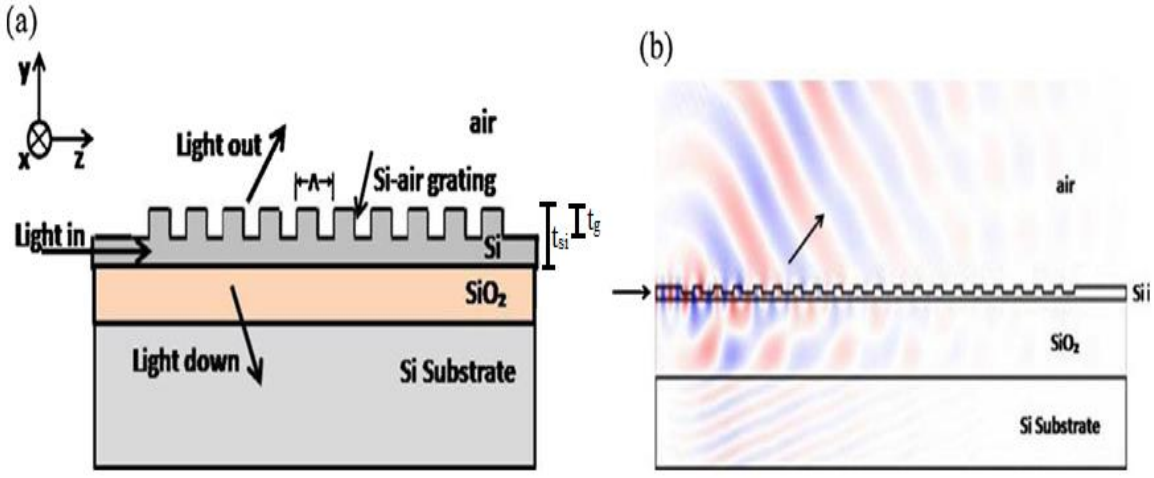

Figure 1.9 (a) Schematic side-view of out-coupler on SOI. t_g is grating-thickness with Si-thickness t_{si} . Λ is the period of grating ; (b) field propagation in out-coupler [27].

(c) High Q resonator

A high-Q resonator with surface-normal emission is used in numerous applications, such as lasers, optical filters, detectors and sensors. In-plane high contrast grating is used to develop high-Q resonator, and to couple light in the surface-normal direction. The attractive property of high-Q resonator with surface normal emission is required, as it will facilitate 99% accuracy with large coupling efficiency for optical fibres[28]. This property is eminent for creation of filters, lasers and good throughput sensor arrays. The *Q*-factor of the resonator is obtained by placing the simulated reflectivity spectra with the Fano-Resonance equation given below [30]

$$R = \frac{r^2(\omega-\omega_0)^2+t^2(1/\tau)^2-2rt(\omega-\omega_0)(1/\tau)}{(\omega-\omega_0)^2+(1/\tau)^2} \quad (1.4)$$

The *Q* factor is given by Eq.1.5

$$Q=\omega_0\tau \quad (1.5)$$

Where $\omega_0 and\ \tau$ are the centre frequency and reso are the centre frequency and resonance lifetime respectively, r and t are are reflectivity and transmittivity coefficients of a uniform slab.

Figure 1.10 shows HCG based high Q resonator. To avoid leakage of light from all four symmetric directions, i.e. ±*x* and ±*z*, the structure consists of distributed Bragg reflectors at the ±*x* ends and below the HCG. The HCG grating comprises of gratings with large number of periods and 3 $In_{0.2}Ga_{0.8}As$ quantum wells placed between $Al_{0.6}\ Ga_{0.4}As$ layers. The end-DBRs are a collection of 1st and 3rd order DBR gratings to ease fabrication process. The air spacing has a width of λ/4, and the semiconductor bar width is 3λ/4. The bottom-DBR comprises 20 pairs of λ/4-thick AlAs/GaAs layers grown on the substrate to reflect the -*z* emission light [28]. A TE-polarized (electric field parallel with the grating) light is excited in the center of the HCG resonator for a short period of time. Energy can be well confined inside the HCG resonator and the output light only emits in the surface normal direction. Further increasing the size of the HCG can result in the improvement of the *Q*-factor.

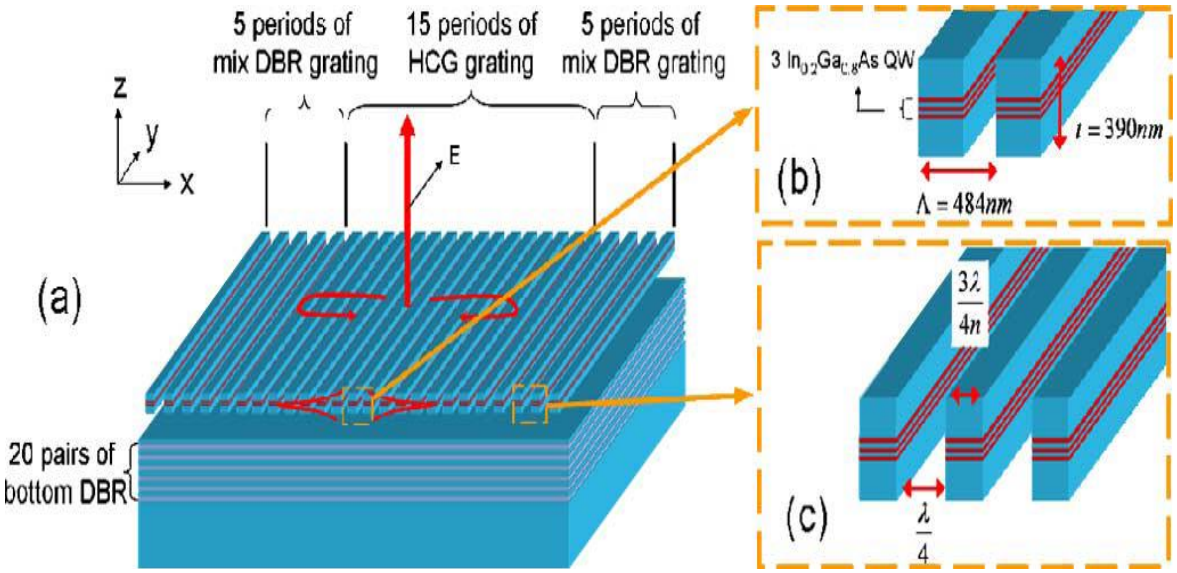

Figure 1.10 (a) Schematic of HCG high-*Q* resonator. (b) Schematic of middle HCG grating with three $In_{0.2}Ga_{0.8}As$ quantum wells embedded inside the grating layer. (c) Schematic of side mix-DBR grating mirror, which is a combination of first-order and third-order DBR gratings [28].

(d) HCG VCSELS

Semiconductor diode lasers play a crucial role in wide range of applications including telecommunication, sensing, solid-state lighting, display and printing. Among various structures, vertical cavity surface emitting lasers (VCSELs) [30-34] are most encouraging, which provides efficient light extraction. The VCSEL has its output light emission perpendicular to the wafer surface and to the plane of the active layers, with the optical feedback provided by distributed Bragg reflectors (DBRs) comprising of many layers of alternating high and low refractive indices. VCSELs have very small gain length, so very high reflectivity (>99%) is required in the DBRs[35]. Due to small index contrast, numerous pair of DBRs is desirable to provide very high reflectivity. The most critical congestion for the realization of VCSELs in large wavelength regions is the availability of materials for making such highly reflective DBRs. With the advancement of optoelectronic devices DBRs are succeeded by a mirror which consists of a single layer of 1-D subwavelength grating made of materials with a high refractive index contrast, known as high-contrast grating

(HCG). This mirror provides many unexplored and unexpected properties that cannot be found earlier in nature[36].

Figure 1.11 shows the schematic of a typical HCG-VCSEL. The device comprises of *n*-DBR mirror that are semiconductor based, an operating wavelength cavity layer with the active region, and an HCG acting as a top mirror. The top mirror consists of two sections: a p-doped DBR and a HCG which is freely suspended. The *p*-DBR helps in spreading current into the active region and preserving the cavity layer during the fabrication process. These *p*-DBR pairs can be reduced or expelled out because a single-layer HCG alone is capable of providing very high reflectivity (R >99.9%) as the VCSEL top mirror. Electric current is injected through the top and bottom contact. An aluminum oxide aperture lies on the upper side of the cavity layer, provides both optical and current confinement [37].

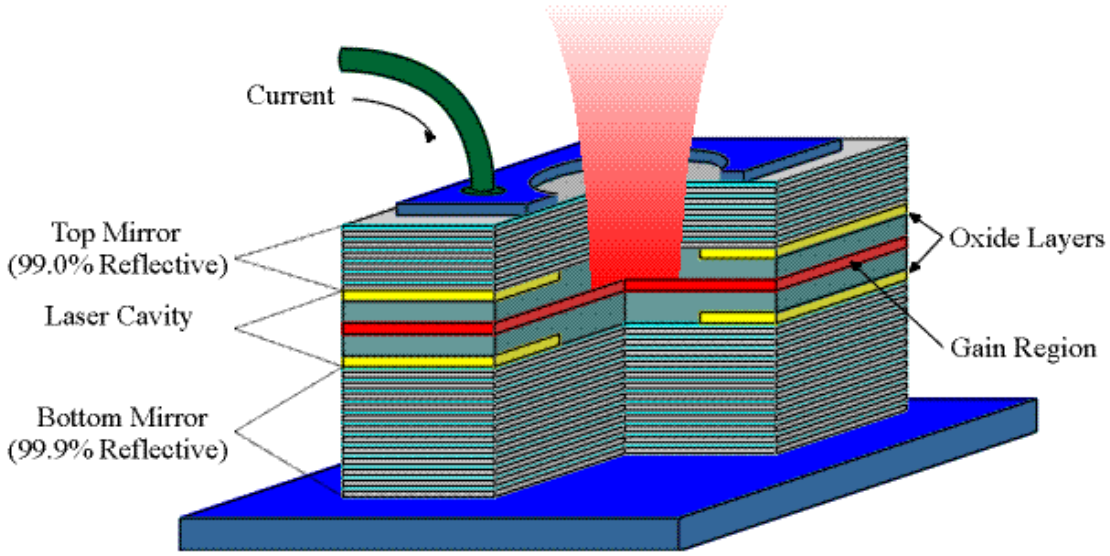

Figure 1.11 Cross-sectional structure of a VCSEL with HCG as a top mirror and 4 pairs of DBRs [37].

1.4 Importance of High Contrast Grating on Silicon-on-Insulator

Silicon-on-insulator (SOI) circuits basically comprises of three elements; an insulating layer (Silicon dioxide, Sapphire, etc.) at the bottom, Silicon layer above it and a final cladding layer on the top. The cladding layer can be Silicon dioxide, air or any other low refractive index material as shown in Figure 1.12. The high index contrast of Silicon (~3.5) and Silicon

dioxide (~1.44) or Air (1.00) permits optimal transmission of electromagnetic waves and reduction of size of photonic devices to great extent. SOI technology [40-42] leads to the decrease of capacitance because of isolation from the silicon substrate that ameliorates power consumption at matched performance. It also lowers leakage current of SOI devices due to isolation, thereby improving the performance of the device. The selection of insulator depends largely on purposive application, with sapphire being used for radiation dependent applications and high performance radio frequency (RF), and silicon dioxide for declining short channel effects in the optoelectronics devices.

Integrated nanophotonics, especially on silicon on insulator (SOI) platform, has recently concede the successful realization of various on-chip nonlinear optical devices. This technology confines the light within sub micro-sized silicon nanowires [43] to increase the optical energy density and allows optical nonlinear effects to occur at diminished input powers. In Silicon photonics, the sandwiched crystalline silicon layer is used to manufacture optical waveguides along with some other passive optical devices such as racetrack resonators, optical multiplexers and demultiplexers. Because of aforementioned differences in the index of refraction, and the fact that Silicon is transparent to infrared light with wavelengths above 1100nm, electromagnetic waves are confined in the waveguides by total internal reflection phenomena.

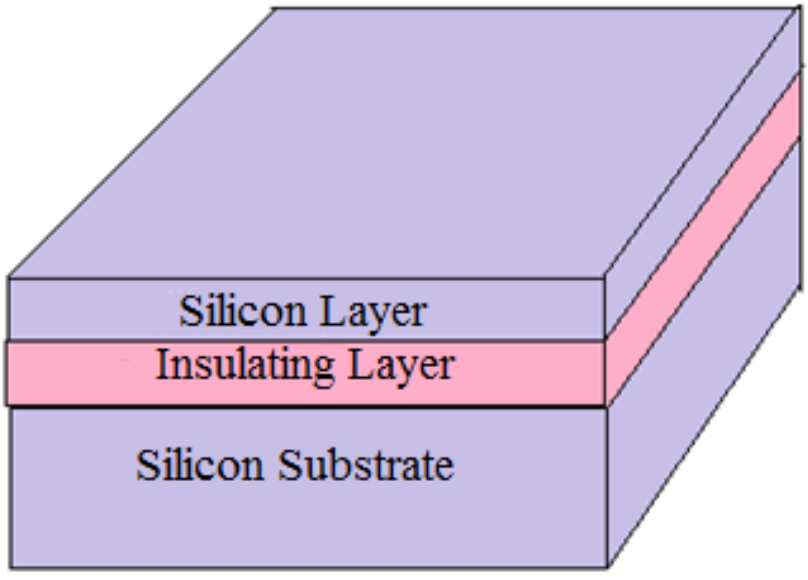

Figure 1.12 Schematic design of Silicon on Insulator (SOI).

The main barrier in the implementation of SOI is the radical increase in cost of the substrate, which further increases the total manufacturing costs. SOI offers high speed, reliability and hardness beyond conventional technologies. Functional structures are developed within the thin crystalline layer, placed over an insulator layer. SOI technology becomes a prime candidate for implementation of hardy, tough and robust circuits for high-temperature operation [42]. Silicon fabrication techniques (CMOS) have become increasingly refined over the past couple decades, motivated by increasing power and efficiency. Currently, SOI technology is not fully developed and is being explored as an alternative to electrical circuits in a variety of applications. It may start replacing CMOS technology once the fabrication cost decreases.

1.5 Terahertz Absorbers

Terahertz range lies in between the microwave and far infrared frequencies; it possesses properties from these regions. Figure 1.13 shows the electromagnetic spectrum. Like microwave, THz waves can penetrate through large number of non-conducting materials like clothing, wood, plastic, paper. Many devices operating in THz range and used for sources, lenses, switches, modulators and detectors do not exist. Also many conventional materials do not respond to this range. THz modulators based on semiconducting structures have broadband nature so they can be used for THz interconnects, but they are only able to modulate a few Percent and usually require cryogenic temperatures[44, 46].

The development of devices and structures with functionality in the terahertz (THz) portion (0.1 to10 THz) of the electromagnetic spectrum is of great importance because of increasing number of applications in sensing and imaging in the THz range, including molecular spectroscopy and medical imaging, short-range wireless THz communication or ultrafast THz interconnects. One of such devices is a THz absorber that has the ability to absorb THz radiation with specific characteristics, including polarization, wide angle, large bandwidth, or multiband capability [47]. THz radiation can be absorbed by some molecules such as DNA and water and these are non-ionizing in nature. These characteristics make THz waves very suitable for numerous applications like environmental monitoring of Earth, medical imaging, and semiconductor electrical property determination and remote sensing of explosives. However, conventional microwave technology cannot measure and detect THz radiation.

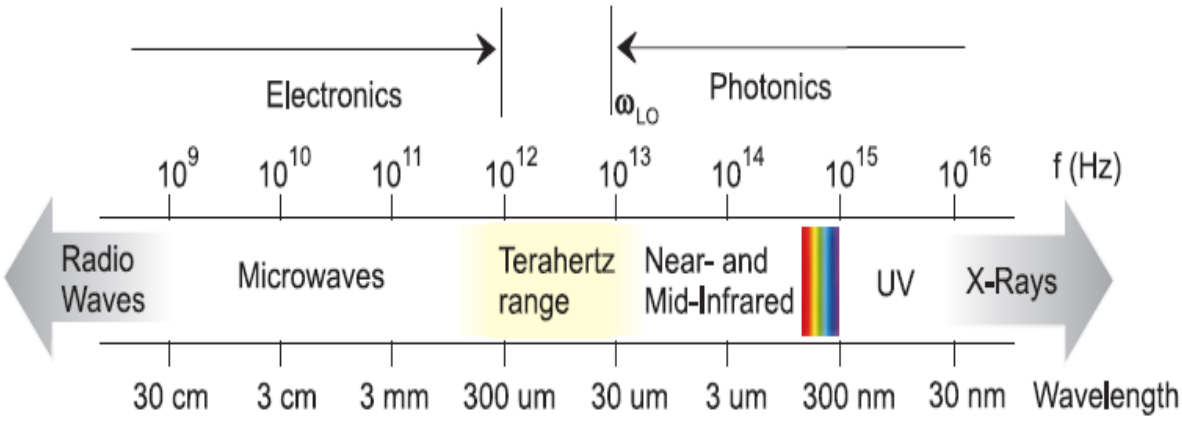

Figure 1.13 Diagram of Electromagnetic Spectrum[45].

Electromagnetic (EM) metamaterials (MMs) are usually defined as a class of artificial media comprises of sub-wavelength metallic or dielectric elements and exhibit exotic EM properties which cannot be found in conventional materials [47]. Essentially, MM is logic concerned with manufacturing of material design, and its capability to obtain non-conventional interactions with EM wave. Metamaterial absorber comprises of the electrical resonator with three or more layers of coupling structures[48]. The electric response in the MA can be achieved from excitation of electric field applied externally by electric resonators, and the magnetic response is obtained from anti-parallel currents on the two sides of the substrate. Thus, the perfect absorption mainly evolved from the strong electric and magnetic resonances simultaneously in an exclusive frequency regime, and provides perfect impedance matching to space based upon the well-known effective media theory. It is feasible to tune frequency range and absorbing characteristics of the Absorber by considering EM properties of dielectric and metallic layers, substrate thickness and shape of the structure. Especially, for THz applications, it is essential to utilize THz absorber with its high performance without compromising with the thermal properties. Thus, the research of the THz Metamaterial Absorber is very attractive [49]. Owing to the perfect absorption of Metamaterial Absorber and its applications, the realization of THz MA with broadband nature is important. However, certain complications are faced in the fabrication of broadband Metamaterial Absorber and is comparatively inaccurate than single layer planar Metamaterial Absorber.

1.5 Purpose and Outline of Work

The purpose of the work is to design and analyze a versatile optical reflector and Terahertz absorber using high index contrast grating on Silicon-on-Insulator (SOI) Chip. Prime focus of the work will be on Silicon-on- Insulator (SOI) based on-chip photonics devices. In this dissertation, design of Broadband Reflector over large wavelength range (1.31-1.76μm) with high Reflectivity (~99%) and Polarization insensitive Broadband Absorber with high Absorption (~98.5%) is proposed that are based on High Index Contrast Grating. Both the designs show large fabrication tolerance. The simulation is done using Rigorous Coupled Wave Analysis method and further validated using OptiFDTD method. This dissertation is divided into following sections.

Chapter 2 discusses survey on the research work done in the High Index Contrast Grating for various practical applications.

Chapter 3 discusses our results on the proposal and analysis of the High Index Contrast Grating structure as a versatile reflector to demonstrate various properties of HCG for VCSELs, including transverse mode control and fabrication tolerance.

Chapter 4 discusses the proposal and analysis of the High Index Contrast Grating based Broadband terahertz Absorber. The structure may serve as a broadband terahertz absorber, which is polarization insensitive and can be used in various practical applications.

Chapter 5 summarizes the whole dissertation with some closing remarks and presents the scope of HCG in near future.

Chapter

2

LITERATURE SURVEY

Papers on Fundamentals of HCG - 2

Papers on HCG based VCSEL - 6

Papers on HCG based Reflector and Mode Control of VCSELs - 6

Papers on HCG based THz Absorber - 7

High-contrast gratings for integrated optoelectronics-2012 [14]

Chang-Hasnain and Yang presented analytical formulation of TE/TM polarized surface normal incidence light on high index contrast grating (HCG) and discussed about phase selection rules of HCG. Some exotic properties of HCG had been discussed which showed that it had created a new platform for novel compact optical devices and facilitated their integration. Characteristics of HCG based VCSELs at 850nm and 1550nm had also been discussed.

Polarization insensitive hollow optical waveguide-2012 [23]

Mukesh Kumar presented polarization insensitive hollow optical waveguide. The propagation characteristics of different modes in the hollow optical waveguide were effectively controlled to provide polarization insensitivity by modifying the HCG thickness and introducing the phase matching layer. The two mirrors-a high-index contrast grating (HCG) mirror and a distributed Bragg reflecting (DBR) mirror were provided on either side of an air-core. A low polarization dependence loss and modal birefringence were achieved.

Low Birefringence and 2-D Optical Confinement of Hollow Waveguide with Distributed Bragg Reflector and High-Index-Contrast Grating-2009 [24]

Mukesh Kumar, et al. presented a design of hollow optical waveguide in which light was confined in an air gap between a bottom mirror as distributed Bragg reflecting (DBR) and a top mirror as high-index-contrast grating (HCG). Because of the combined effect of periodicity of both the mirrors, the proposed hollow waveguide showed a small modal

birefringence at narrow air core and also provided strong 2-D optical confinement. The acceptable propagation loss of TE mode had also been presented.

A novel ultra-low loss hollow-core waveguide using subwavelength high-contrast gratings-2009 [29]

Ye Zhou, et al. presented a novel design of low loss hollow core waveguide using high contrast grating, which would serve as a building block in many on-chip photonic devices including optical sensors, delay lines, interconnects. Low propagation loss could be achieved using both RCWA and FDTD. HCG-HW reduced non linear effects and dispersion in transmitted data and thus becomes the prime candidate for on-chip communication.

A surface-emitting laser incorporating a high-index-contrast subwavelength Grating-2007 [30]

Michael C.Y. Huang, et al. demonstrated VCSELs incorporating high contrast grating as a top mirror. The versatility, wavelength scalability and flexibility of the single-layer HCG design could provide numerous advantages when fabricating surface normal optoelectronic devices, such as high-brightness LEDs, detectors and photovoltaic cells, micro-electromechanical and optical filters (MEMS) tunable devices, for a wide range of wavelengths. Low threshold current, polarization insensitivity and single transverse mode in VCSELs had been observed.

Size effect of high contrast gratings in VCSELs -2009 [32]

Christopher Chase, et al. showed through simulations and experiments the variation of the size of HCG incorporated in tunable VCSELs. The properties of VCSELs were shown to be independent of size of HCG. This helped in increasing the tuning speed of optical devices which enabled attractive applications in wavelength tunable optoelectronic devices, detectors and filters.

1550 nm high contrast grating VCSEL -2010 [33]

Christopher Chase, et al. demonstrated VCSEL operating at 1550nm incorporating high contrast grating(HCG) which was electrically pumped (HCG) and exhibits proton

implantation to form electrical apertures. At room temperature it has >1mW output power. The structure provided single mode operation with large apertures and there would be no degenerate polarization modes. These found attractive applications in optical communication systems. Dielectric mirror deposition or additional re-growth was not needed for the fabrication of the devices rather it required monolithic epitaxial growth.

High-Contrast Grating VCSEL-2009 [34]

Connie J. Chang-Hasnain et al. presented recent advancements in HCGs. The design of HCG based VCSEL, its fabrication, optical properties, transverse and polarization mode control of VCSELs has been discussed. The basic concepts and characteristics of tunable VCSEL were demonstrated. Tunable VCSELs integrated with HCG as a reflectivity mirror had led to decrease in the tunable mirror size and improvement in tuning speed. This would help in monolithic integration of HCG in optoelectronic devices for large wavelengths.

Long-Wavelength High-Contrast Grating Vertical-Cavity Surface-Emitting Laser-2010 [35]

Werner Hofmann, et al. presented a novel design of vertical-cavity surface-emitting laser (VCSEL) integrating HCG as the output mirrors and hybrid reflector as a bottom mirror for high speed modulation. The structure provided polarization stability and single mode operation by suppressing higher order modes at longer wavelengths in an elegant way. This found interesting applications in high speed data transmission in optical domain mainly for passive optical networks.

Large Fabrication Tolerance for VCSELs Using High-Contrast Grating-2009 [36]

Ye Zhou, et al. demonstrated experimentally a large fabrication tolerance of single-layer, highly reflective HCG incorporated in vertical cavity surface emitting lasers as a top mirror. Both uniform and non uniform geometries of gratings had been investigated. For non uniform grating geometry, larger variations in the dimensions of HCG could be accepted. This made the devices suitable for WDM applications and decreases the cost of optical devices.

High-Index-Contrast Grating (HCG) and its Applications in Optoelectronic Devices-2009 [37]

Ye Zhou, et al. presented recent advancements and various applications of HCGs in optical devices, including VCSELs, modulators, tunable VCSELs, high-*Q* optical resonators, detectors and low-loss hollow-core waveguides (HWs). HCGs could function as broadband, high-reflectivity (>99%) mirrors for surface-normal incident light, shallow angle reflector which was useful to replace conventional distributed Bragg reflectors in optical devices and helped not only in reducing the size of optoelectronic devices but also increased their performance.

High-contrast gratings as a new platform for integrated optoelectronics-2011 [38]

Connie J Chang-Hasnain discussed the manipulation of light by high index contrast grating to obtain exotic properties. Various designs to achieve broadband high reflectivity mirrors and high Q- resonator with surface normal or oblique emission were discussed to replace heavy and discrete optics. A number of applications were discussed in optoelectronic devices including low loss hollow core waveguides, VCSELs, Tunable VCSELs. HCG based low loss, planar, high-numerical aperture, focusing reflectors and lenses were presented which could be incorporated in a variety of integrated photonic and electronic devices.

Enhanced absorption and optical force in a sandwiched grating at the terahertz band-2013 [44]

Yong Zhang, et al. presented a design of multiband terahertz absorber with multiple high absorption peaks over a wide range of incident angles in the terahertz frequency regime (0.1-10 THz). The structure showed strong positive or negative electromagnetic force induced by resonances in grating that can be tuned by modifying the grating parameters. This effect could be utilized in a variety of applications including mechanical oscillation of terahertz devices and thus increases the opto-mechanic coupling in the THz regime.

Engineering heavily doped silicon for broadband absorber in the terahertz regime-2012 [45]

Mingbo Pu, et al. presented the design of a broadband terahertz absorber using silicon grating which is heavily doped by boron. Doping might change the concentration of charge carriers

in grating semiconductor material which leads to tunable structure with THz excitations. To increase the operating bandwidth, the period of grating was so well chosen that zero and first order diffraction came nearer in frequency. The design could be readily extended to higher frequencies by only varying the properties of the subwavelength grating by changing the doping concentration.

Highly flexible wide angle of incidence terahertz metamaterial absorber: Design, fabrication, and characterization-2008 [47]

Hu Ta, et al. presented the design, and characterization of a metamaterial narrowband absorber with high absorption at terahertz frequencies i.e. an absorption of 97% at 1.6 THz could be obtained. The main advantage of the device was its small size which found attractive use in non- planar applications. Metamaterial absorber provided large absorption over a wide range of incident angles for both TE and TM configurations.

Perfect Metamaterial Absorber-2008 [49]

N.I. Landy, et al. presented the design of metamaterial absorber using two metamaterial resonators with very high absorption over a narrow frequency range. Absorption was achieved due to the ability of the meta materials to absorb electric and magnetic components of incident light. The design was polarization sensitive which limits its usage in various optoelectronic devices. Metamaterial absorber application in bolometer had been discussed. It had been shown that metallic absorption was inappropriate in comparison to dielectric absorption or any other losses.

Wide-angle perfect absorber/thermal emitter in the terahertz regime-2009 [51]

Marcus Diem, et al. demonstrated perfect absorber using metallic nanostructures which exhibited very high absorption over a wide range of angles. The structure could be tuned by modifying the dimensions of nanostructure. It also demonstrated the stability of the device with respect to the change in material parameters with the change in temperature. This device could be used for microwave experiments as it avoided reflections.

Broad-Band Mirror (1.12–1.62 μm) Using a Subwavelength Grating-2004 [54]

Carlos F. R. Mateus, et al. demonstrated a novel design of broadband mirror using single-layer subwavelength grating (SWG) over a wide reflection spectrum ranges from 1.12–1.62 μm and provided very high reflectivity (98.5%) under normal incident. This subwavelength grating was scalable for different wavelengths by modifying the grating parameters, which facilitated monolithic integration of optoelectronic devices over a wide range of wavelengths. The structure provided application for active and passive devices including tunable VCSELs, microelectromechanical devices and focal plane arrays.

Narrow band, large angular width resonant reflection from a periodic high index grid at terahertz frequency- 2012 [57]

Olivier Parriaux et al. presented ultra-narrow band reflector with large angular width in the terahertz frequency range on a single-crystal silicon grid using a thin silicon grating of definite depth and width under normal incidence. THz time-domain experimental demonstration of narrow band reflection was presented. It had been experimentally proven that zero transmission leads to 100% reflection. Resonant reflection effect based on modes propagating up and down the grating slits had been analyzed.

Narrow band resonant grating of 100% reflection under normal incidence 2006 [58]

N. Destouches, et al. presented a narrow band reflector with very high reflection using multilayer sub mirror (DBR) and a waveguide sub mirror (HCG) that provided zero transmission. The structure exhibited very narrow linewidth, polarization insensitivity and low propagation loss which made the device to be used in disk lasers. Different applications of resonant mirrors were also presented. Methodology had been provided which enabled the design of various optical devices that operated at different wavelengths and made from different materials.

Transverse Mode Control of VCSELs Using Angular Dependent High-contrast Grating Mirror-2013 [60]

Junichi Kashino, et al. demonstrated the transverse-mode control of VCSELs at 980nm using HCG mirrors. The fabricated Silicon HCG showed the large angular dependence of reflectivity, fundamental mode propagated at very small angles with very high reflectivity

whereas higher order modes propagated at larger angles with much lower reflectivity. So by using the angular dependence property of HCG transverse mode control of VCSELs had been achieved.

Polarization Mode Control in High Contrast Subwavelength Grating VCSEL-2008 [61]

Michael C.Y. Huang, et al. demonstrated polarization mode control in VCSEL incorporating a single-layer high-index-contrast subwavelength grating as a top mirror under both CW and pulsed operation. HCG not only provided high reflectivity but also provides mode selectivity in VCSELs which further decreases the polarization dependent noise in optical links that were based on VCSELs.

Monolithically integrated multi-wavelength VCSEL arrays using high-contrast gratings-2010 [62]

Vadim Karagodsky, et.al. presented novel design of multi-wavelength array of HCG based VCSEL. A range of VCSEL cavity wavelengths could be obtained by altering only the period and filling factor of the high-contrast gratings, without changing the epitaxial layer thickness. This novel design could easily accommodated the entire Erbium-doped fiber amplifier bandwidth which could be applied to fabricate multiwavelength filters and detectors. There was no restriction on physical layouts for emitted wavelengths.

Theoretical Investigation of Broadband and Wide-Angle Terahertz Metamaterial Absorber-2014 [64]

Ben-Xin Wang, et al. demonstrated metamaterial broadband terahertz absorber with very high absorption (>99%) over a large range of incident angles up to 50˚. The broadband absorption originated from longitudinal coupling of modes between stacked layers which could be further enhanced by increasing the number of layers. This could be extended to other higher frequency regimes to increase its usage in various applications like solar cell, detection and imaging.

Chapter 3

Proposal and Analysis of High Index Contrast Grating as a Versatile Optical Reflector

3.1 Structure of High Index Contrast Grating

Subwavelength gratings having a large refractive index contrast give rise to a new class of planar optics. This subwavelength grating is known as High Contrast Grating (HCG). The schematic of the subwavelength high index contrast grating based on SOI is shown in Figure 3.1. The structure consists of air/silicon grating (a high index media surrounded by low index media) on top of SOI chip. The three important design parameters are: grating height, duty cycle and grating period which are denoted as *h, η* and *p* respectively. Duty cycle is ratio of width of the high index bar to the grating period. The TE/TM polarized light is incident onto the Air/Silicon grating at different angle of incidence. Simulations are done by using RCWA (Rigorous Coupled Wave Analysis) and CAMFR (Cavity Modeling Framework) [52].

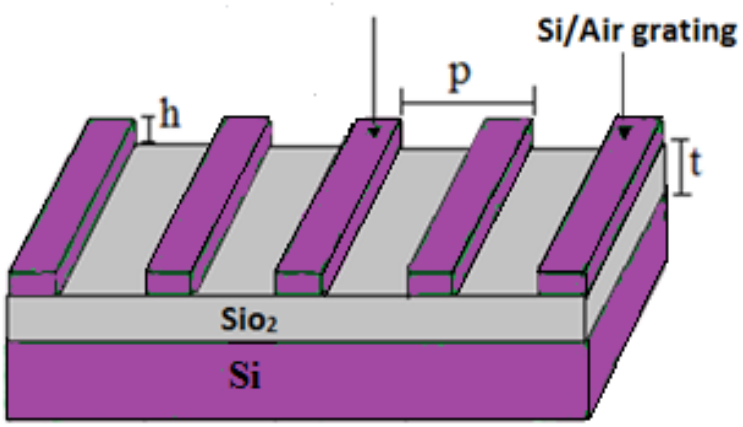

Figure 3.1 Schematic of subwavelength high index contrast grating based on a silicon-on-insulator (SOI) chip. The incident light is TE/TM polarized which is incident at surface normal direction.

This extremely simple structure provides exotic properties and it is as thin as 15% of operating wavelength. It is fabricated to reflect or transmit partially or completely depending on the application with specific optical phase over various incident angles. Spatially chirped

HCGs serve as an excellent focusing reflectors and high numerical aperture lenses. Not only at surface normal direction but also at oblique angles of incidence, HCG shows remarkable properties. HCG resembles DBR and 1D photonic crystals by its physical structure. But the uniqueness of HCG comes from the interaction of waveguide array modes.

HCG Reflectivity matrix R can be obtained from Eq.4.1 which is common in transmission line theory:[53]

$$R = (Z_{in} + I)^{-1}(Z_{in} - I) \tag{4.1}$$

where Z_{in} is the normalized input impedence matrix similar to constant in transmission line theory:

$$Z_{in} = E(I + \varphi\rho\varphi)(I - \varphi\rho\varphi)^{-1}H^{-1} \tag{4.2}$$

ρ is the reflection matrix which relates the two coefficient vectors of E or H field and φ is the HCG propagation matrix which contains the accumulated phases of HCG mode. E and H are the electric and magnetic field profiles respectively. The HCG reflectivity and transmission, and the relation between the two in the subwavelength regime, are given by Eq. 4.3

$$\text{HCG Reflectivity} = |R|^2$$

$$\text{HCG Transmittivity} = |T|^2$$

$$\text{For SubwavelengthGratings where } p < \lambda$$

$$|R|^2 + |T|^2 = 1 \tag{4.3}$$

Simulations At Near Infrared Range(0.9µm-10µm)

3.1.1 HCG as A Surface Normal Broad-Band Mirror (1.31–1.76µm)

BROAD-BAND mirrors[54] with very high reflectivity (>99%) are crucial for many practical applications, including telecommunications, imaging, surveillance, and sensors. The DBR, which comprises of many layers of alternating materials having periodic variations of indices, is widely used as high-reflectivity mirror in most surface-emitting lasers. Due to small index contrast, numerous DBR pairs are required to achieve high reflectivity that can be achieved by using only single layer of HCG due to its high index contrast. Large number

of DBR pairs led to epitaxial growth challenges in many material systems. Metal mirrors have high absorption losses so they are not suitable for the production of transmission devices. HCG is scalable for different wavelengths by modifying only the grating parameters, which facilitate on-chip integration of devices over a wide range of wavelengths. The dielectric layer below the grating is important for the mirror effect[55]. The higher the index-contrast, larger the reflection bandwidth can be obtained. The HCG mirrors have attractive applications in many active and passive devices like visible and infrared wavelength VCSELs, micro-electromechanical tunable devices, and reconfigurable planar arrays.

The design parameters for the simulation of structure includes the materials involved (index of refraction (n)), thickness of the dielectric layer below the grating (*t*), period (*p*), grating height (*h*), and duty cycle. Figure 3.2 shows the reflectivity spectra of HCG when TM polarized light is incident on the grating from surface normal direction and the optimized parameters are: Si substrate having index n=3.48 (Si), low index material has refractive index =1 (air), n_l= 1.47 (SiO_2), *h* = 0.46µm, thickness of dielectric (*t*)=0.8 µm. The period and duty cycle are taken as 0.7 µm and 0.75 respectively. A very high reflectivity (>99.5%) spectrum, ranging 1.31µm to 1.76µm is obtained using RCWA method.

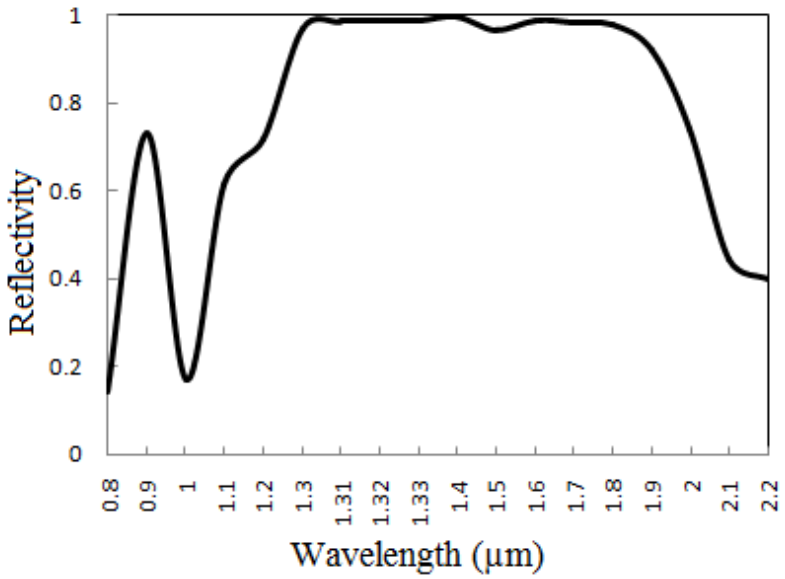

Figure 3.2 Simulated reflectivity spectra for surface normal incident TM polarized light on SOI HCG structure using RCWA method with grating period (p) = 0.7 µm, thickness of dielectric (*t*) =0.8 µm ,grating height (h)= 0.46 µm, duty cycle (η) =0.75 .

3.1.2 HCG as A Narrow-band Mirror

HCG can also be designed to act as a narrow-band mirror or a high-*Q* resonator[56-58] by properly choosing the dimensions such that the average energy in the propagation direction is nearly zero at both the front and rear interfaces of the grating. A narrow-band mirror designed for 1550 nm is presented here. The grating high-index material has refractive index as 3.48 at 1550 nm. The low-index material is taken as 1. The grating is designed for TE-polarized light. The HCG parameters are grating period (Λ) = 0.8μm, thickness (t) = 0.55 μm, and duty cycle (η) = 0.74. The reflectivity spectrum of the HCG structure is simulated using CAMFR[52], as shown in Figure 3.3. A reflectivity graph having a sharp asymmetric line shape with reflection varies from 0 to 1 for a narrow wavelength range is achieved. The high reflectivity under normal incidence and narrowest reflection peak at 1.55μm with 100% reflectivity is achieved in order to choose a single longitudinal mode. This function is required in second harmonic generation and interferometer.

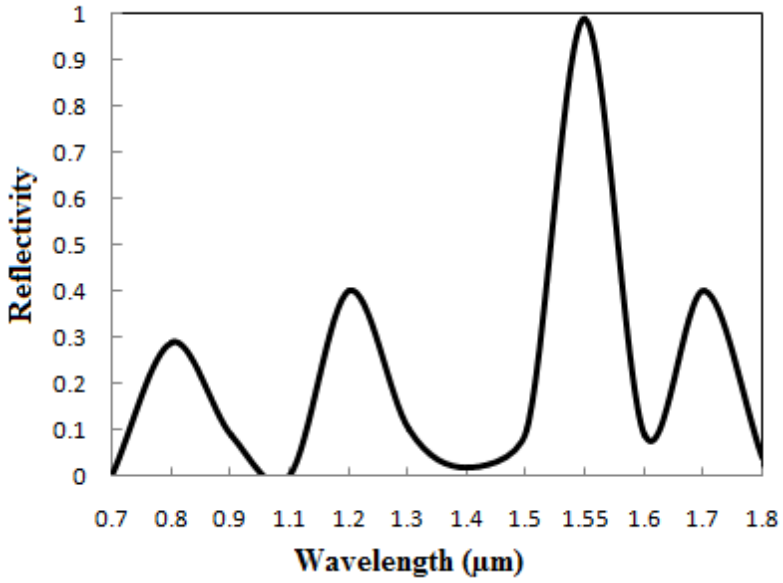

Figure 3.3 Simulated Narrow-band reflected spectra for TE- HCG with grating period (Λ) = 0.8μm, thickness of dielectric (t) = 1 μm, grating height (h)=550 nm, duty cycle (η) = 0.74.

3.1.3 Transverse Mode Control Using HCG

To achieve high performance in optical communication systems, a single mode operation with a fundamental transverse mode is essential [59-61]. In order to achieve single mode operation with high output power, extra loss structures (passive antiguide region, photonic

crystal defects and shallow surface relief) can be introduced to suppress the higher order transverse modes from lasing. But these methods increase the structure complexity and decreases fabrication tolerance.

Due to its engineered angular dependence, HCG is used to suppress higher order transverse modes and helps in achieving a single mode, hence enhances the performance of optical devices by providing high output power. Figure 3.4 shows the reflectivity of HCG when TM polarized light is incident at different angle of incidence. Figure 3.4 also shows that the transverse angle for each transverse mode is different; a fundamental mode has the smallest transverse angle with much larger reflectivity (~99%) while the high-order modes have larger angles and provides low reflectivity (~40%). Thus it is easy to select only a fundamental mode using the highly angular dependence nature of HCG. This avoids all the higher-order modes to propagate and enhances the light output. The optimized parameters in this simulation are: height of grating and dielectric thickness is 290 nm and 500 nm respectively. Grating period is 455 nm, a duty cycle is 0.68 (solid line) and 0.75 (dotted line) at fixed wavelength of 980nm.

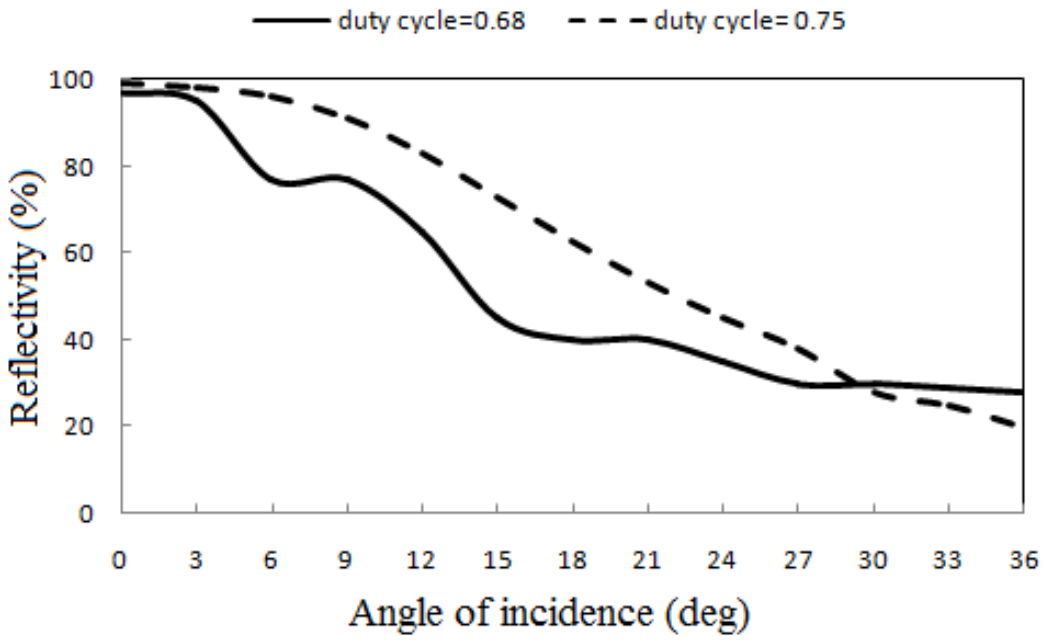

Figure 3.4 Simulated angular dependence characteristic of HCG for the transverse mode control at fixed wavelength of 980nm with grating parameters: grating height = 290nm, thickness of dielectric = 500nm, period=455nm, duty cycle= 0.68(solid line) and 0.75 (dotted line)

3.1.4 Near Field Characteristics

Figure 3.5 shows the near field optical characteristics of the light wave emitted from HCG when TM polarized light is normally incident on it. Despite the fact that the grating is rectangular, the emitted light wave remains symmetrical, and possesses Gaussian profile for the fundamental mode. The beam is measured to be about 2μm, which is characterized by the width of the 99% decrease in intensity. The near field intensity distribution for a TE-HCG is similar to TM-HCG.

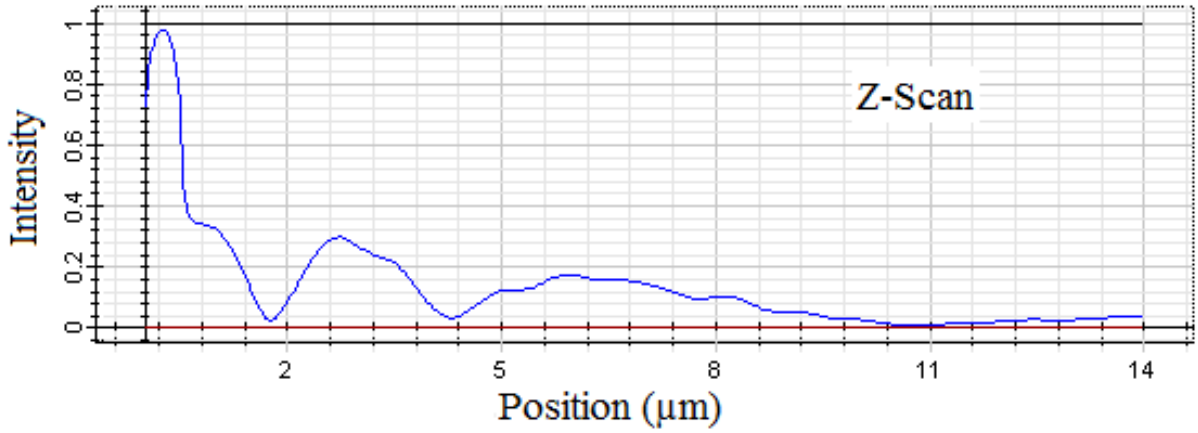

Figure 3.5 Measured optical near-field characteristics of the TM-HCG for VCSEL incorporated with HCG as top mirror. The output beam emitted from HCG has Gaussian profile.

3.1.5 Large Fabrication Tolerance

The fabrication tolerance of different parameters in the HCG structure is simulated using RCWA method. The contour plot in Figure 3.6 shows the fabrication tolerance of HCG in terms of grating height, where wavelength is varied from 1.25 μm to 1.8 μm while other design parameters period, thickness of dielectric layer, duty cycle is kept fixed at 0.7μm, 0.8μm and 0.75 respectively. The HCG structure can have grating height variation from 300 nm to 460 nm, and still provides high reflectivity (>99%). Figure 3.7 shows the fabrication tolerance of period of HCG when wavelength is varied over a large range. The other parameters i.e. grating height and duty cycle are kept fixed at 0.46 μm and 0.75 respectively. A 50-nm variation in grating period (~10% of the design period of 450 nm), while still providing very high reflectivity (>99%) for the wide range of wavelengths for the VCSELs to

lase if used in it as a top mirror. This leads to the large fabrication tolerance in HCG-VCSEL fabrication. The large fabrication tolerance of the HCG structure originates from its broadband nature and wavelength scalability. By modifying the dimensions of HCG, the reflectivity spectrum of the HCG can be scaled accordingly to obtain a high reflectivity for a particular wavelength. So HCG is a covetable broadband reflector with high reflectivity and having large fabrication tolerance for VCSEL applications.

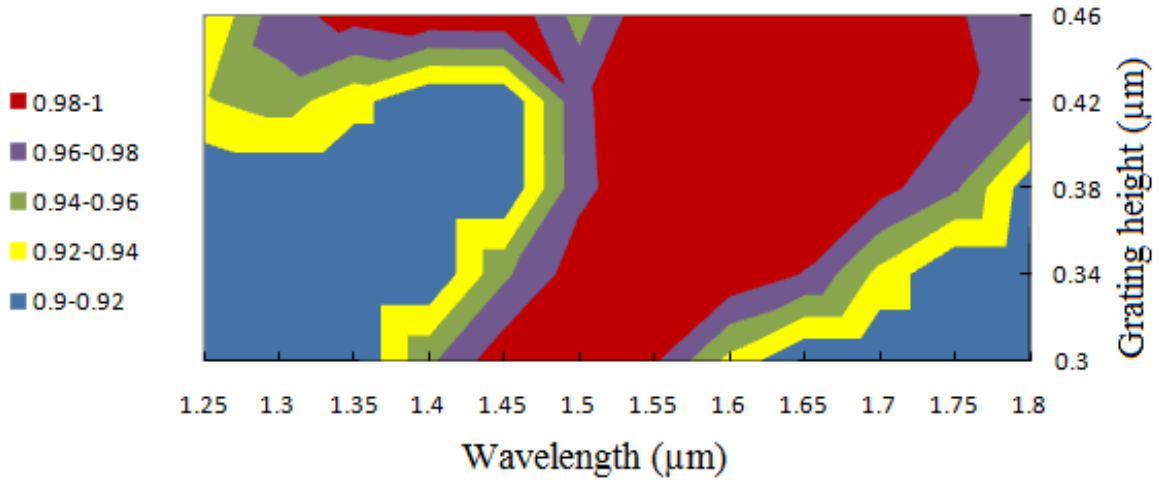

Figure 3.6 Fabrication tolerance for HCG height, which is more than 160 nm for (>99%) reflectivity. Duty cycle is 0.75 and period is kept fixed at 0.7µm. The thickness of dielectric layer below the grating is 0.8 µm.

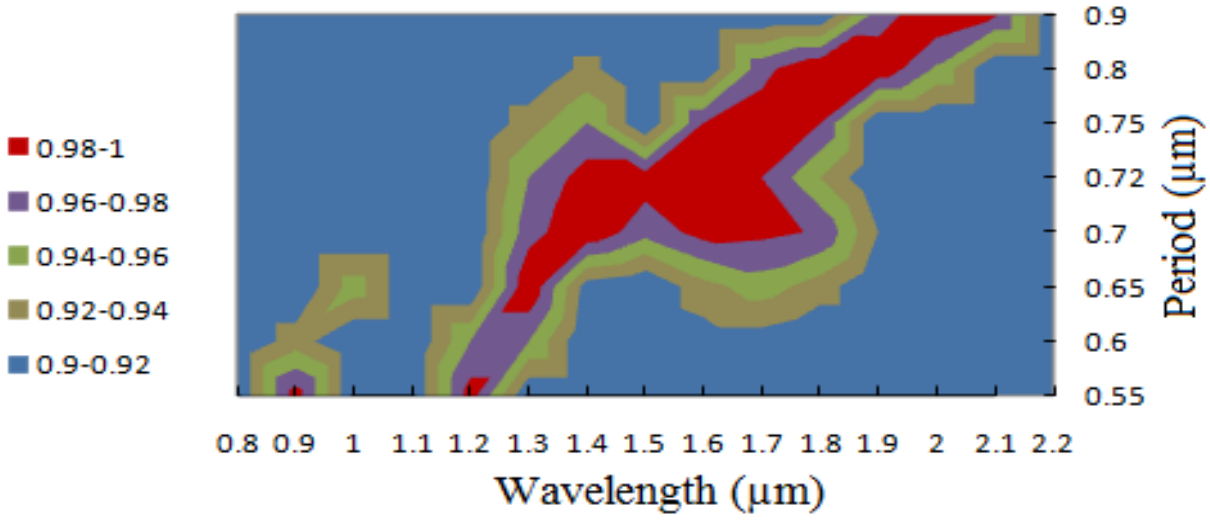

Figure 3.7 Fabrication tolerance for HCG period, which is more than 50nm for (>99%) reflectivity. Duty cycle is 0.75 and Thickness of dielectric layer below the grating is 0.8 µm, grating height is kept fixed at 0.46 µm.

3.1.6 HCG as a Multiwavelength VCSEL Array at Near IR (1.0μm-1.8μm)

High contrast gratings have been employed in many optoelectronic devices. It has been integrated in VCSELs as a reflectivity mirror. The light weight of HCG provides fast electromechanical structure actuation for tuning the wavelength. The increasing demands of high bandwidth applications, such as real-time video conferencing or online video streaming have become motivation for high capacity data networks. Wavelength Division Multiplexing (WDM) offers best way to hold high bandwidth of an optical fiber while using existing electronics. Figure 3.8 shows the schematic of multiwavelength VCSEL array. Multiwavelength and monolithically integrated sources [62] are extremely covetable for wide range of applications including optical displays, optical trace-gas sensing etc. The phase of HCG reflectivity is dependent on dimensions of grating which leads to wide range of its emission wavelengths.

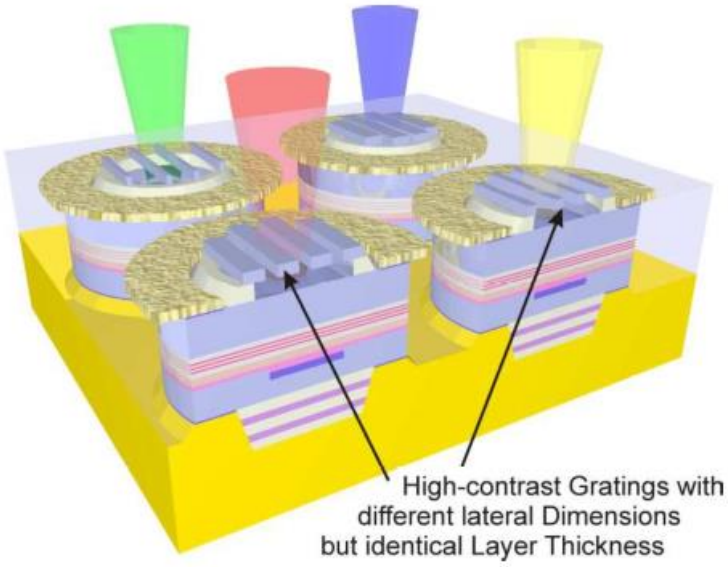

Figure 3.8 Schematic of multiwavelength VCSEL array [62].

Figure 3.9 shows the reflectivity spectra of HCG structure at different duty cycles. It shows that at duty cycle 0.85 multiple peaks are obtained with very high reflectivity (>99%) and this makes the device tunable for wide range of wavelengths. At duty cycle 0.8, a broadband spectrum is obtained and at duty cycle 0.95, less number of peaks with very high reflectivity is obtained. Figure 3.10 shows the multiwavelength nature of HCG, which depicts that it can be well tuned for wide range of wavelengths. Simulation is done using CAMFR. The

optimized parameters in this simulation are: Si substrate (n=3.48), (p) = 0.6µm, low index material having index=1 (air), n_l= 1.47 (SiO_2), h = 0.45 µm and duty cycle =0.85. Thickness of dielectric is 1 µm.

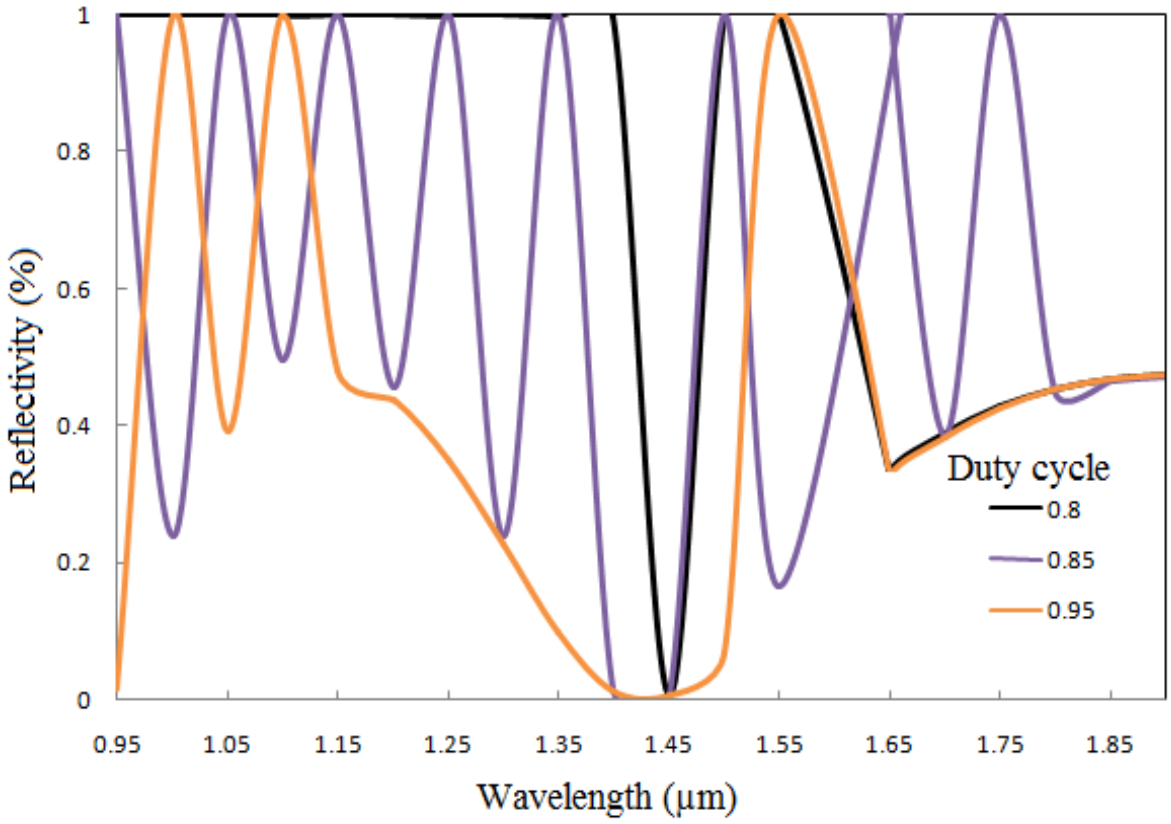

Figure 3.9 Simulated multipeak spectra using HCG at normal incident for TE wave having period=0.6µm and varying duty cycle.

The VCSEL wavelength is determined by round-trip 2π phase condition as in any Fabry-Perot cavity:

$$4\pi {L_{cavity}}/{\lambda_{lasing}} + \emptyset_{HCG} + \emptyset_{DBR} = 2m\pi \qquad (4.4)$$

L_{cavity} is the length of the cavity, λ_{lasing} is the lasing wavelength. $\emptyset_{HCG} and\ \emptyset_{DBR}$ are the reflectivity phases of HCG and DBR mirrors respectively and m is any integer. To obtain a large wavelength range in λ_{lasing} , design of HCG is required whose $\emptyset_{HCG}$ is varied with period and duty cycle.

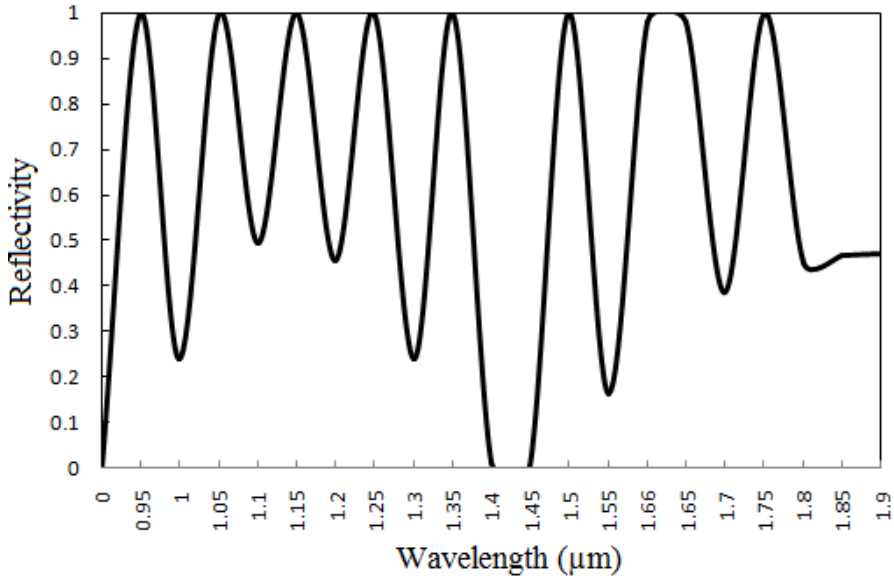

Figure 3.10 Simulated reflectivity multiwavelength spectrum of HCG with grating period (p) =600nm, grating height (*h)* =450 nm, duty cycle (η) =0.85, for normal incident TE polarized light**.**

Simulations At Mid Infrared Range (10µm-100µm)

3.2 HCG as a Narrowband Transmission Filter at Mid IR (8µm-14µm)

The principle of reflectance is that the incident light is coupled to the guided modes in the dielectric grating waveguide, where strong coupling corresponds to broadband response and weak coupling corresponds to narrowband response. This physical principle is used to realize a narrowband transmission filter[63] using a single-layer dielectric grating. This characteristic of HCG is useful for filtering applications including military surveillance, remote sensing. The optimized parameters in the simulation shown in Figure 3.11 are: Si substrate (n=3.48), (*p*) = 5µm, *h* = 3 µm and *t* = 4.6 µm. Period and duty cycle are 5 µm and 0.72 respectively. θ is the incident angle with the surface normal direction to the grating. Figure 3.11 also shows the two narrow peaks, first peak having transmittivity (~60%) and second first peak is having transmittivity (~72%) for angle of incidence as 5˚. Figure 3.12 shows the Transmittance as a function of increasing wavelength when light is incident at surface normal direction on HCG. Single Transmittance peak is obtained with very low value of transmittivity (~50%) means broadband reflection can be obtained at surface normal incident. Grating Parameters are same as above.

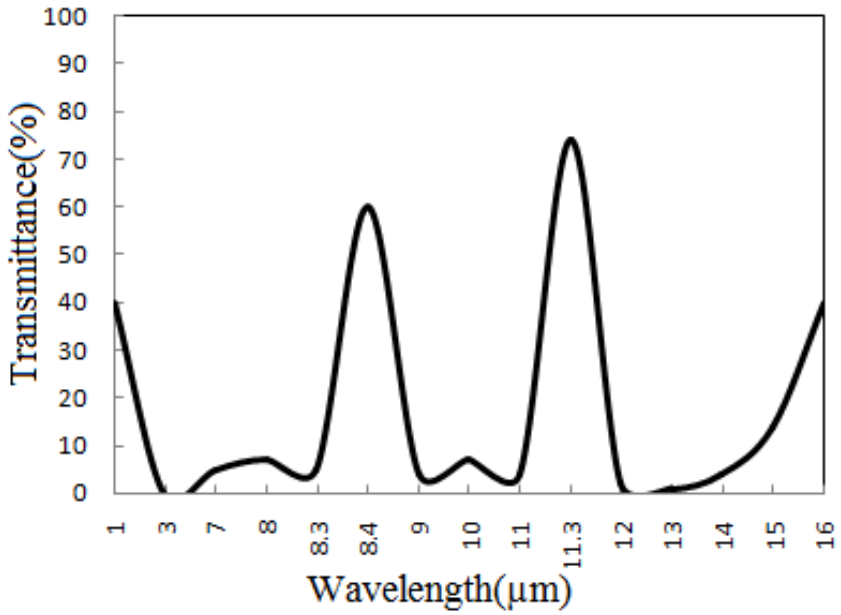

Figure 3.11 A line plot of transmittance as a function of increasing wavelength for TM polarized wave incident at an angle θ = 5º.Grating height is 3µm and thickness of middle layer (air) is 4.6 µm. Period and Duty cycle are 5 µm and 0.72 respectively.

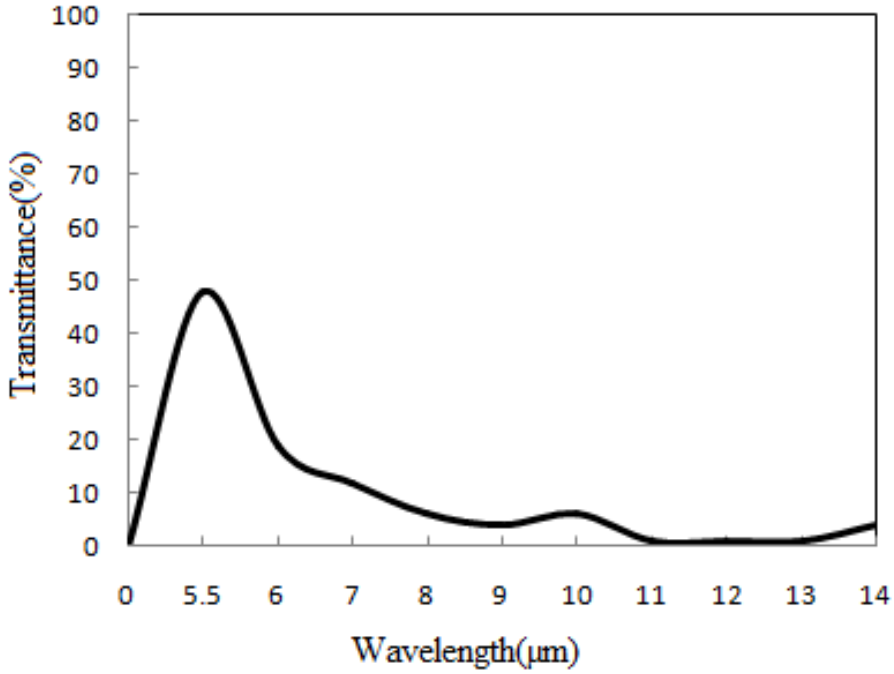

Figure 3.12 A line plot of transmittance as a function of increasing wavelength at Surface normal Incident. Grating height is 3µm and thickness of middle layer (air) is 4.6 µm.Period and Duty cycle are 5 µm and 0.72 respectively.

Figure 3.13 (a) ,(c) shows the Magnetic field profiles associated with each transmission band on each resonance peak that are shown in Figure 3.11, depicting the supported modes at θ=5º. By introducing the off normal incidence, the response of broadband reflector has changed. The off-normal response exhibits well-defined transmission bands, within the broadband. Figure 3.13 (b) shows the single period of high index contrast grating. First resonant peak obtained in Figure 3.11 is having comparatively less transmittance so more light is confined in the grating region as shown in Figure3.13 (a), while second peak is having high transmittance so less light is confined in grating region as shown in Figure 3.13 (c).

Due to large Fabrication tolerance of HCG, the variations in the grating height and dielectric thickness as 4±0.5 μm and 4 ± 0.2μm respectively can be tolerated. Although the filter is simulated in the thermal emission spectrum (8 - 14 μm), the same principle is also valid at higher frequencies, including the optical regime, in which the desired frequency range is selected by modifying the grating dimensions.

3.2.1 Improved Structure for Narrowband Transmission Filter Using HCG

In the above case, air is taken as dielectric between silicon grating and substrate. But practically it is very much difficult to fabricate the device with air as dielectric as grating which is suspended in air. In the proposed design silica is used in place of air. This structure is not only easy-to-fabricate but also increases the transmittance to 96% whereas in earlier case it is only 70%.

The optimized parameters in this simulation are: Si substrate (n=3.48), (p) = 5μm, n=3.48 (Silicon), low index material is having the index =1 (air), n_l= 1.0 (air), h = 4.1 μm and duty cycle (ff) = 0.70 and middle layer thickness (t) =5.4μm and θ is angle of incident with the surface normal direction of the grating. The incident wave is TM polarized and incident at 5˚ with the surface normal direction. Figure 3.14 shows the three transmission peaks with high transmittivity at an incident angle θ= 5º. Figure 3.15 depicts magnetic field profile associated with the transmittance peak occur at wavelength of 11.3 μm. Less light is confined in the grating region due to large transmittivity at this wavelength.

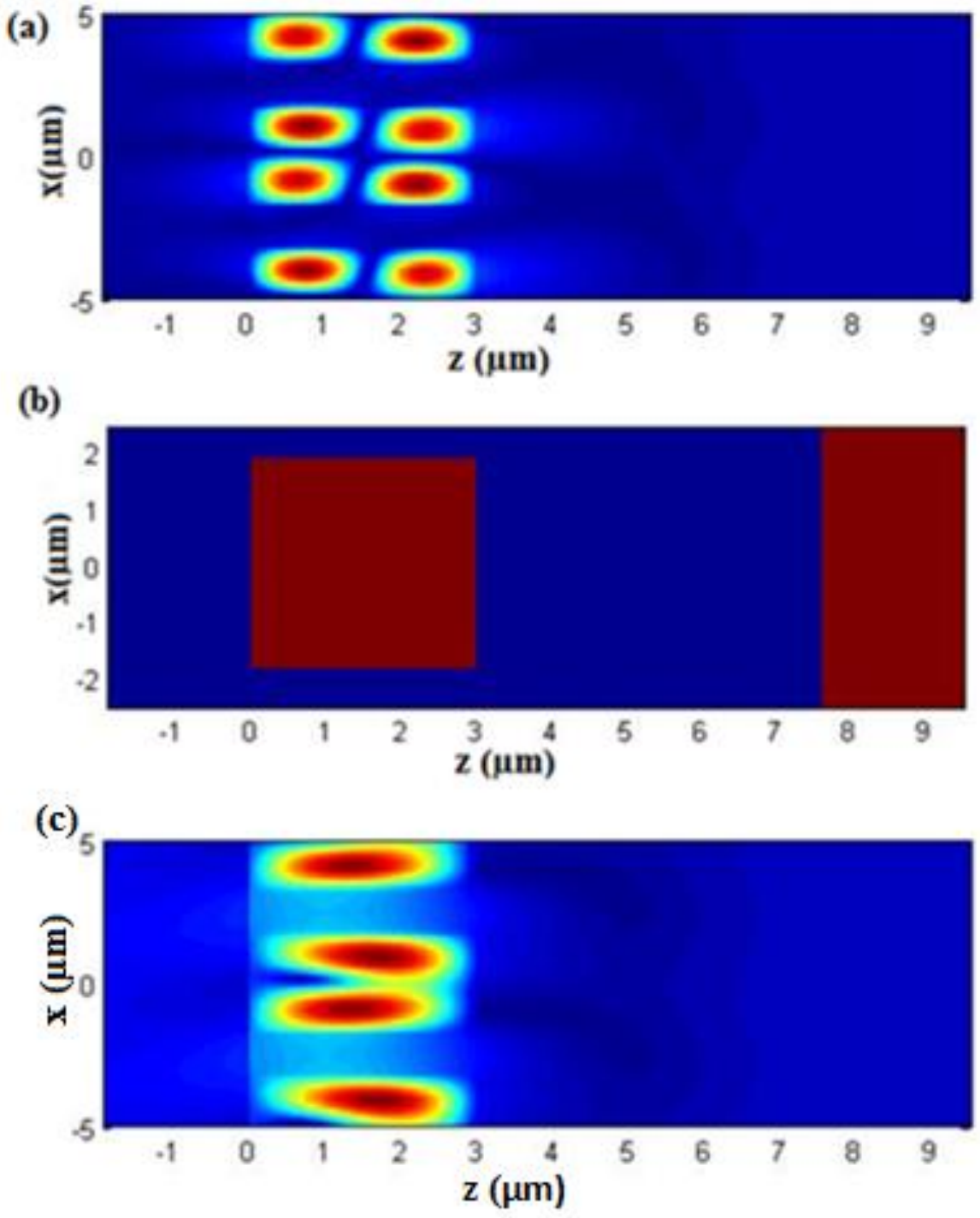

Figure 3.13 Simulated response of the optimized suspended silicon grating with period=5µm, ff=0.72, t= 4.6µm , h= 3µm (a) Magnetic field profiles, on first resonance showing the supported modes at θ=5º (b) Single period of HCG (c) Magnetic field profiles, H_z , on second resonant peak showing the supported modes at θ=5º.

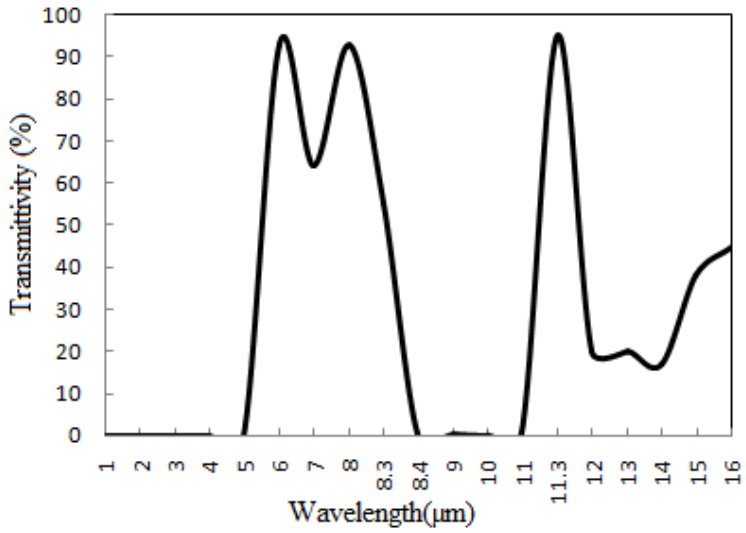

Figure 3.14 A line plot of transmittance as a function of increasing wavelength at incident angle θ= 5º using silica as middle layer of thickness 5.4μm. Grating height is 4.1 μm. Incident light is TM polarized and incident at an angle of 5˚ with the surface normal direction.

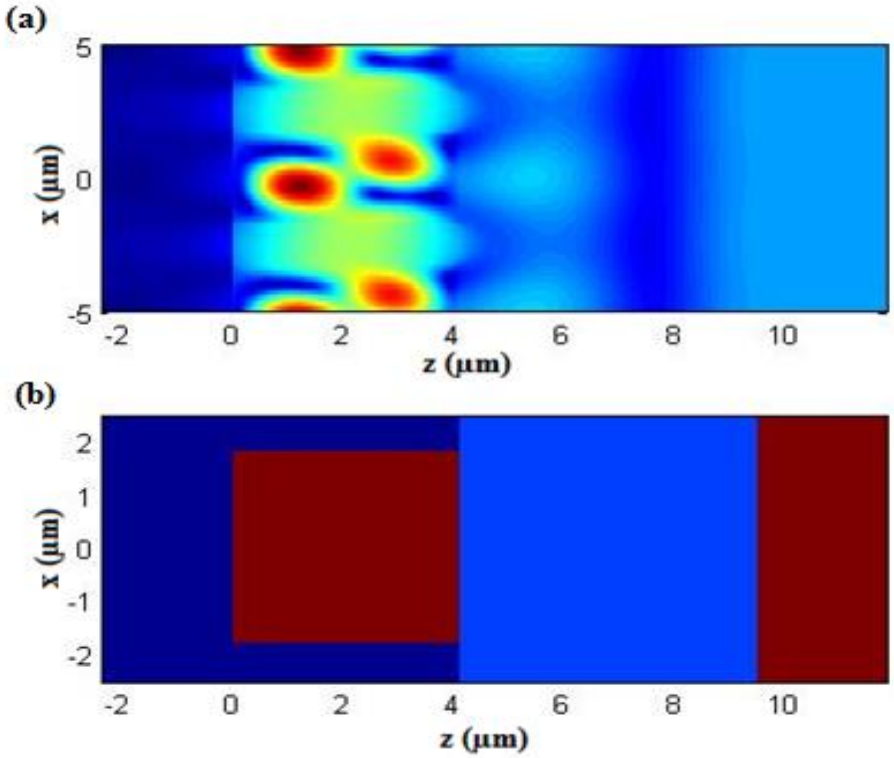

Figure 3.15 Simulated response of the optimized silicon/Air grating with period=5 μm, ff=0.70, t= 5.4μm, h= 4.1μm (a) Magnetic field profiles, on first resonance showing the supported modes at θ=5º (b) Single period of HCG.

Summary of the Chapter

In this Chapter, the broadband property and fundamental physics related to the working of high index contrast grating (HCG) is discussed. More than 98.5% reflectivity has been demonstrated by simulation over a large wavelength range of 1.31-1.76μm, which is desirable in many optoelectronic devices. Additionally, HCG can serve as narrowband mirror at telecom wavelength and multiwavelength device having large fabrication tolerance, thus helps in monolithic integration of many photonic devices. Narrowband Transmission filter using HCG with transmittivity larger than 97% has been simulated.

Chapter

4 Proposal and Analysis of Broadband Terahertz absorber on SOI Chip

4.1 Structure of Absorber

The schematic of the proposed absorber design is shown in Figure 4.1(a). It consists of a silicon/air high-index contrast grating (a high index media surrounded by low index media) on top of a SOI chip. The two important design parameters that control the absorptivity are: grating height and grating period which are denoted as *h* and *p* respectively. Another design parameter is duty cycle which is the ratio of width of the high index bar to the period of grating. It is noticed that the high absorption at a particular wavelength results in trapping of the resonant light in the structure due to FP resonances and thus decreases reflectivity and increased absorptivity. After the absorption of the incident terahertz radiation the proposed engineered SOI chip guides the terahertz waves in the grating region in form of in-plane oscillations as shown in Figure 4.1(b). The field propagation on the SOI chip is computed using CAMFR (CAvity Modelling FRamework) tool [50].

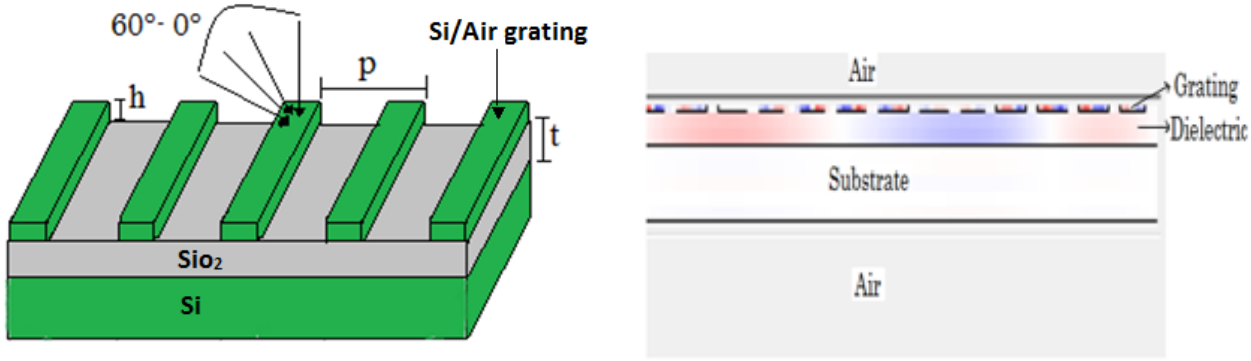

Figure 4.1 (a) Schematic of the broadband and wide-angle terahertz absorber with high-index contrast grating. A thin dielectric separates a silicon substrate and a silicon/air high-index contrast grating. The incident light is TM polarized at different angle of incidence from 0˚ to 60˚ (b) Field propagation in grating region of the terahertz absorber simulated using CAMFR simulation tool when TM polarized light is normally incident on it.

4.2 Absorption Characteristics

HCG is a subwavelength grating i.e. period is much smaller than the operating wavelength, so only zeroth order mode will propagate and all higher order modes are evanescent modes. Due to its 1-D periodic nature, HCG is polarization sensitive. When light is incident on the grating, large number of eigen-modes get excited and start propagating towards the bottom of grating interface with different phase velocities. At the exiting plane, due to a strong mismatch (index contrast) to the existing plane wave, the waveguide modes reflect back and also couple with each other. Similar mode coupling happens when modes guides and arrives back to the incident plane. The reflectivity is obtained by considering modes through one complete round. The HCG parameters are well chosen that these modes get destructively interfere at the bottom of grating interface. This yields zero Transmission coefficient [60] and the incident light gets absorbed if there is no reflection.

All the design analysis are performed with RCWA [38] which analyses the diffraction of an electromagnetic plane wave incident on subwavelength grating which is surrounded by two different media. Figure 4.2 shows that the grating is periodic and infinite in y direction and uniform and infinite in x direction. In the *z*-direction it is divided into three regions: upper region of grating is Region 1 having refractive index n_1, grating region is Region 2 and lower region of the grating is Region 3 having refractive index n_2.

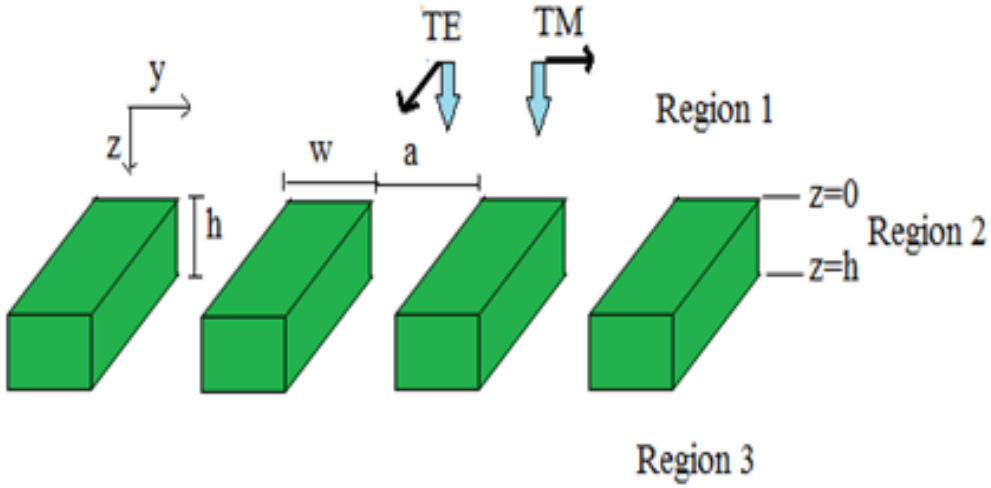

Figure 4.2 High-index Contrast Grating Schematics, The blue arrow shows incident wave and black arrows corresponds to E-field Direction in both TE/TM polarizations of incidence. *w* is width of the Silicon stripe and *a* is width of air gap. The grating height (*h)* is taken in *z* direction.

As the grating periodicity is in *y* direction, diffracted wave vector in *y* direction is given by [19]

$$K_{i,y} = K_{in,y} + i\frac{2\pi}{p} \tag{4.1}$$

Where $K_{in,y}$ is incident wave vector, k_0 is wave vector in vacuum, K is grating wave number given by $(\frac{2\pi}{p})$ .When TE polarized light is incident onto the grating at angle (θ) with the normal, the normalized incident electric field vector is

$$E_0 = \exp(-jk_0 n_1(ysin\theta + zcos\theta)) \tag{4.2}$$

The diffracted magnetic and electric field from the grating

$$H_1 = e^{-jkz} - \sum_{i=0}^{\infty} R_i H_{y,i}^1 e^{+j\gamma_i z} \tag{4.3}$$

$$E_1 = E_0 + \sum_i R_i \, exp[-j(Kyi\, y - K1, zi\, z)] \tag{4.4}$$

$$H_3 = \sum_{i=0}^{\infty} T_i H_{y,i}^3(x) e^{-j\gamma_i(z-h)} \tag{4.5}$$

$$E_3 = \sum_i T_i \, e\, xp\{-j[K_{yi}y - K_{2,zi}(z-h)]\} \tag{4.6}$$

$$K_{yi} = K_0[n_1 sin\theta - i(\lambda p)] \tag{4.7}$$

Where *i* is diffraction order number, R_i and T_i are reflection and transmission coefficients, γ_i is propagation constant, $K_{yi}$is *y* component of *i*-th wave vector, $K_{1,zi}$ is *z* component of *i*-th wave vector in Region 1. E_1 and E_3 are diffracted electric field from the grating in Region 1 and Region 3 respectively. The magnetic field and Electric field in Region 2 is given by

$$H_2 = \sum_{i=0}^{\infty} H_{y,i}^2(x)[a_i e^{-jk(z-h)} - b_i e^{+jk(z-h)} \tag{4.8}$$

$$E_2 = \sum_i S_{xi}(z)\exp(-jK_{yi}y) \tag{4.9}$$

$$\nabla^2 E_2 + (^{2\pi}/_{\lambda})^2 \in (y,z)E_2 = 0 \tag{4.10}$$

a_i and b_i are the coefficients of the forward (+z) and backward (-z) propagating constants respectively.

λ is free space wavelength. S_{xi} is normalized amplitude of *i*-th wave vector in Region 2 that can be obtained by substituting Eq. (4.1- 4.9) in wave Eq. (4.10).The solution of Eq. (4.10) can be obtained in terms of eigen-values and eigen-vectors. The reflection and transmission coefficients can be obtained from Eq. (4.11) and (4.12) respectively. The coefficients C_m can be determined by matching tangential electric and magnetic fields at the two boundaries (*z*=0 and *z*=*h*). ω_{im} is the *m*-th element of row in matrix [ω], that consists of all eigen vectors corresponding to *i*-th wave. Absorption can be achieved by using Eq. (4.10)

$$R_i + \delta_{i0} = \sum_m C_m \omega_{im} \tag{4.11}$$

$$T_i = \sum_m C_m \omega_{im} \exp[j(q_m \mathsf{C} - \varepsilon_{2i}(h)] \tag{4.12}$$

The Absorption coefficient of *i*-th wave vector A_i is given as

$$A_i = 1 - T_i - R_i \tag{4.13}$$

where $\delta_{i0}$is kroneckar delta function, q_m is *m*-th eigen value, ε_{2i} is positive real for propagating wave and negative imaginary for evanescent wave and C is coupling coefficient.

The results are obtained using RCWA where the proposed structure is illuminated by a normally incident polarized plane wave. To enhance the absorption, the period of the grating structure should be 2.5% of the wavelength used, so that only the zeroth order mode may propagate and all others are the evanescent modes [62]. The *T* is very close to zero as the thickness of the dielectric is much larger than its skin depth; *A* may approach unity i.e. perfect absorption can be achieved when *R* is close to zero.

Figure 4.3 shows the effect of grating height *h* and period *p* on the absorption of incident terahertz radiation. The absorption remains high, more than 90%, over a long range of grating period from 20 μm to 45 μm where the operating wavelength is 74 μm and the grating duty cycle is 0.72. The grating height from 2 μm to 3.5 μm provides absorption of larger than 90% over a long range of grating period from 20 μm to 45 μm. It is to be noted from the Figure 4.3 that the fabrication tolerance of the absorber is quite large in terms of grating height and grating period. The absorption remains large over wide range of both the design parameters. At *h* = 2.6 μm and *p* = 27 μm, a high absorption of 98 % is achieved.

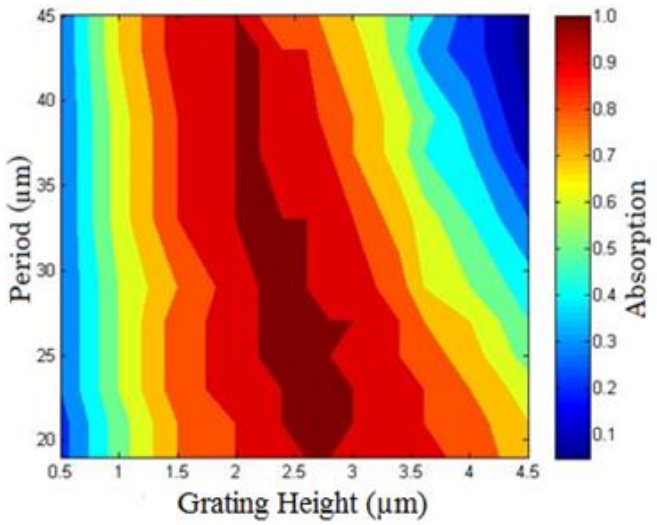

Figure 4.3 Variation of terahertz absorption with grating height and grating period. Duty cycle of the grating is 0.72 at fixed wavelength of 74 µm. The height of grating and the thickness of dielectric are 2.6 µm and 4.8 µm.

Figure 4.4 depicts the effect of grating period on the absorption-bandwidth of HCG based SOI chip. It is to be noted that the bandwidth of high absorption (from 90 % to 98 %) is quite large over a wide range of values of grating period. The grating height (*h*) is 2.6 µm and thickness of dielectric (*t*) is 4.8 µm and duty cycle is 0.72. The absorption is high (~98%) over a long range of period from 12 µm to 35 µm.

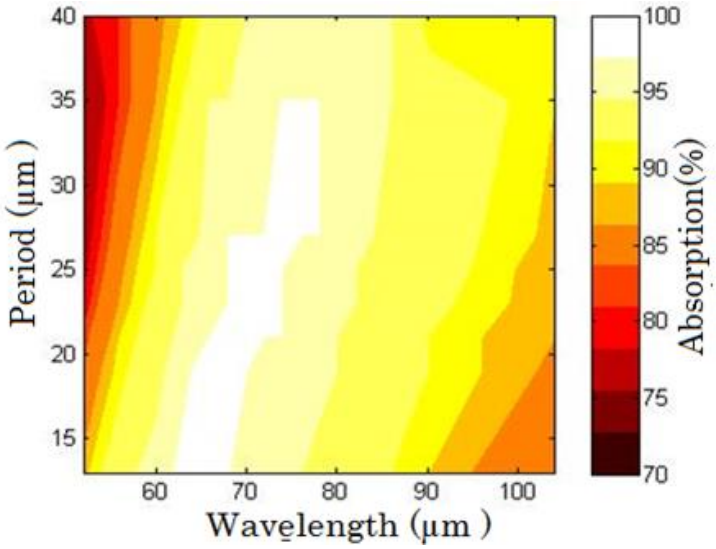

Figure 4.4 Effect of grating period on absorption bandwidth at duty cycle = 0.72 and h=2.6 µm and t=4.8 µm. The fabrication tolerance of the absorber is large as the absorption remains large over a wide range of values of grating period.

The grating period is the most critical parameter while fabricating a grating. The reflection properties of a grating are sensitive to any change in grating period. To increase the fabrication tolerance of the grating based device it is necessary to make the output characteristics of the device unchanged for a wide range of grating period. It is also clear from Figure 4.4 that the fabrication tolerance of the proposed absorber is large enough (14μm period tolerance for grating height as 2.6 μm) for practical applications. Figure 4.5 shows the broadband absorption spectra where a high absorption above 98% is achieved over a wavelength range of 66μm-84μm with grating height 2.6 μm and dielectric thickness 4.8 μm. Period and Duty cycle are 27 μm and 0.72 respectively. At p = 27 μm the bandwidth of high absorption (>98%) from 66 μm to 84 μm is achieved.

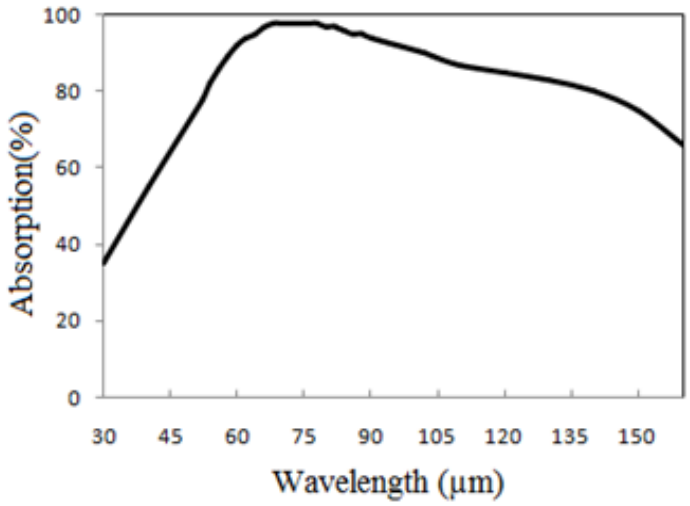

Figure 4.5 Absorption spectra for HCG on SOI with Grating parameters- period, duty cycle, thickness of dielectric are 27 μm, 0.72, 4.8 μm respectively. Grating height is 2.6 μm.

In many applications, electromagnetic wave is incident onto the absorber with an oblique incident angle, so it is desirable to make device which can operate on a wide range of incident angles [63]. An absorber with narrow accepted angles has limited usage in practical applications. Figure 4.6 shows the behavior of the proposed structure at different angle of incidence on absorption spectra. It shows that the broadband absorption (greater than 98%) is not limited to normal incidence (0°) but can be extended to 60°. Thus, the designed absorber provides large absorption over a wide range of incident angles [64]. A high absorption (>98%) over a wide range of incident angles from 0° (normal incidence) to 60° is obtained.

This wide angle broadband characteristic arises from the wideband nature of HCG. The grating height is 2.6 µm, dielectric thickness is 4.8 µm, period is 27 µm and duty cycle is 0.72.The light incident on the grating is TM polarized.

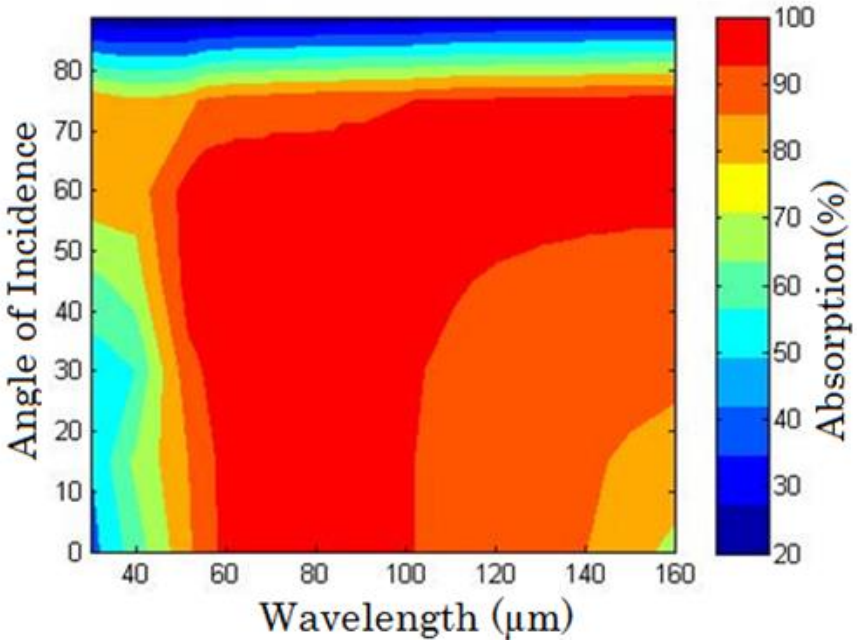

Figure 4.6 Dependence of absorption spectra on angle of incidence, design parameters are h = 2.6µm, t = 4.8 µm, duty cycle = 0.72, p = 27 µm.

4.3 Polarization Dependence

The propagation characteristics of the two orthogonal polarizations (TE: E-field parallel to the grating lines and TM: E-field orthogonal to the grating lines as shown in Figure 4.2) in the absorber are effectively controlled in simulation to provide polarization insensitivity by transfiguring the parameters of the structure. Flexibility in designing an HCG helps in fabricating large number of photonic devices [62-64]. Figure 4.7 Shows absorption of two orthogonally polarized waves at different wavelengths. Dimensions are same as that of broadband absorber i.e. h = 2.6 µm and t = 4.8 µm. Period (p) is 27 µm and duty cycle is 0.72. Here the polarization dependent absorption PDA (the difference in absorption of TE and TM mode) is large (~31%). For perfect polarization independence of a terahertz absorber, the PDA must be small enough. Presence of HCG on SOI can make it possible to reduce the polarization dependence resulting from the high-index contrast in the grating and

strong in-plane alterations of the guided waves in the grating [62]. To reduce the PDA for the realization of polarization insensitivity of the absorber, the grating height, thickness of dielectric and period values are optimized. The duty cycle is kept same i.e. 0.72. Figure 4.7 (b) shows the effect of varying period on Polarization dependent Absorption (PDA) when thickness of the dielectric is taken as 3 μm at fixed wavelength 54 μm. Duty cycle is 0.72. The PDA is lowest (0.1%) at grating thickness 2μm when period is varied from 20 μm to 25 μm and it is also low for h = 0.5 μm. Figure 4.7 (b) also shows large fabrication tolerance of the device by providing low PDA when grating height is varied from h=0.5 μm to h=2 μm.

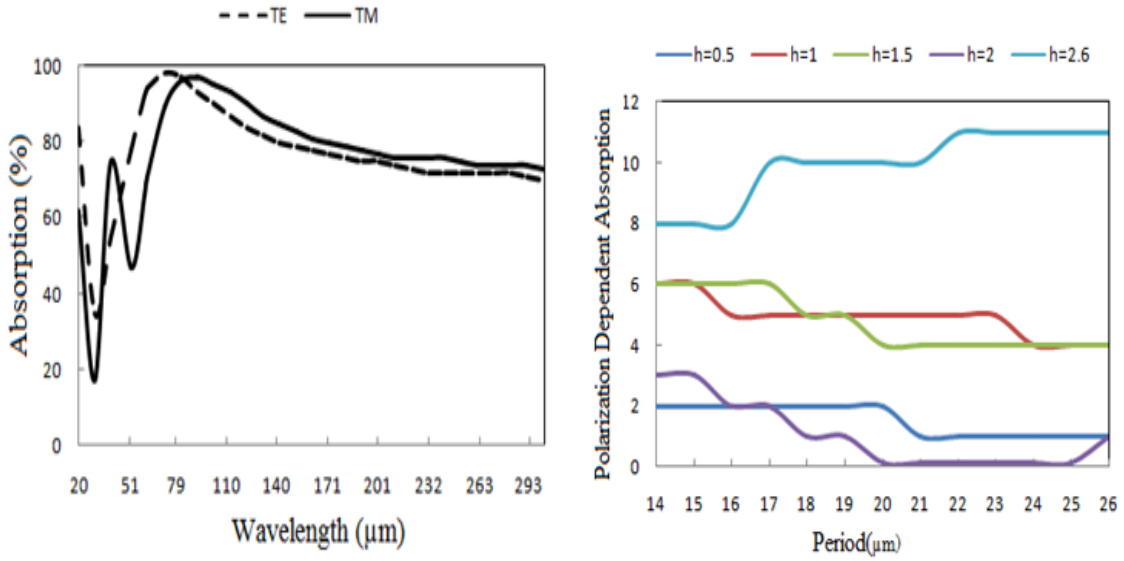

Figure 4.7 (a) Absorption spectra for TE (dotted line) and TM (solid line) polarizations with grating height 2.6 μm and dielectric thickness 4.8 μm with period 27 μm and duty cycle 0.72; (b) the effect of variation of grating period on polarization dependent absorption (PDA) at fixed dielectric thickness of 3 μm and operating wavelength of 54 μm. Duty cycle is kept at 0.72.

Figure 4.8 shows absorption spectra for both TE and TM polarized light after minimizing the difference between the two modes i.e. after realization of low PDA (0.1%) to make the device polarization insensitive. To minimize the difference between two orthogonal polarizations, the grating height, dielectric thickness and period are altered and taken as 2 μm, 3 μm and 20 μm respectively. This is necessary to achieve polarization insensitivity because some optical components change the polarization state of transmitted light in an uncertain manner and sometimes the optical source of radiation itself emits an unpolarized light.

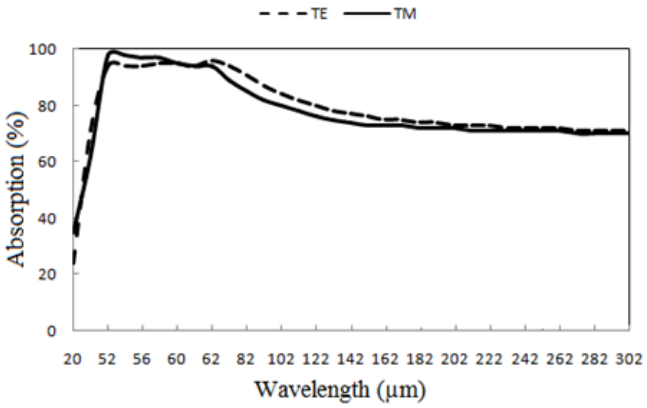

Figure 4.8 Absorption spectra for TE (dotted line) and TM (solid line) polarized light with grating height 2µm and dielectric thickness 3µm with period 20 µm and duty cycle 0.72.

4.4 Validation of Results with FDTD

The design of the proposed terahertz absorber is validated with the FDTD method. Figure 4.9 shows the absorption of terahertz waves as a function of grating period. The results are calculated using RCWA as well as using FDTD. The grating parameters are: duty cycle is 0.72, grating height is 2.6 µm and thickness of dielectric is 4.8 µm. Wavelength is kept fixed at 74 µm. The results obtained with the RCWA are in good agreement (with maximum difference of 0.6% in absorption) with those obtained with FDTD. Figure 4.9 also clarifies the large fabrication tolerance of the proposed design i.e. 8µm period tolerance with ~98% absorption.

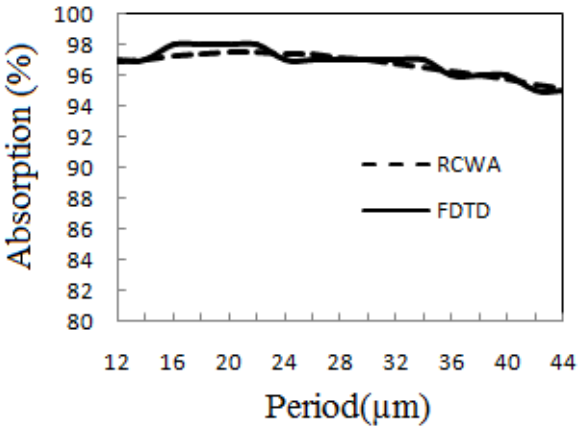

Figure 4.9 Validation of RCWA designed absorber with FDTD method, absorption versus grating period using RCWA and FDTD at duty cycle =0.72, grating height = 2.6 µm and thickness of dielectric = 4.8 µm at fixed wavelength of 74 µm.

Chapter 5

Conclusion and Future Scope

This dissertation targets at the design, simulation and analysis of a single layer subwavelength high-index contrast grating on silicon-on-insulator chip. In this proposed work, it has been shown that by modifying the three basic parameters i.e. grating height, period, duty cycle of HCG, many useful and yet previously unobtainable properties can be achieved. It discusses how HCG can manipulate light and behave as Broadband reflector and Absorber over a large frequency range with very large fabrication tolerance. This shows that HCG can be readily incorporated in a variety of integrated optoelectronic and photonic devices. HCG can serve as a Broadband reflector over a wavelength range of 1.31-1.76μm, narrowband Reflector at 1550 nm with very high reflectivity i.e. 99%. The simulation results are presented to demonstrate many desirable characteristics of HCG for VCSELs, including polarization selection, near field characteristics, large fabrication tolerance and transverse mode control.

Lastly, the design of an efficient terahertz absorber on an engineered SOI platform based on a 1-D high-index contrast grating is presented. The design and analysis are carried out using RCWA. A high absorption (> 98.4%) over a frequency range of 3.57 - 4.54 THz is obtained with large fabrication tolerance (14μm period tolerance for grating height of 2.6μm). The absorption remains high (~ 98 %) for wide range of angle of incidence from 0˚ (Normal incidence) to 60˚. The results obtained by RCWA are in good agreement (with maximum difference of 0.6%) with that obtained by FDTD. Results shown by this simple geometry are the wealth of its interesting properties. The presence of HCG on SOI can make it possible to reduce the polarization dependence resulting from the high-index contrast in the grating and strong in-plane modifications of the guided waves in the grating region. The large fabrication tolerance originates from the wavelength scalability of HCG. The structure may serve as a broadband terahertz absorber, which is polarization insensitive and can be used in various practical applications. By adjusting the physical dimensions of subwavelength Febry perot

cavity, the absorption can be achieved over a larger terahertz spectrum. This simple device may provide a desirable absorption method and operation to select frequency band in high frequency region for many useful applications in realizing terahertz devices. A further broadening of the absorption bandwidth is also possible (by using doped silicon instead of bare silicon) to readily extend it to other frequency regimes for a host of applications for imaging, micro-electro-mechanical tunable devices and stealth technology.

References

[1] Mauro J. Kobrinsky, Bruce A. Block, Jun-Fei Zheng, Brandon C. Barnett, Edris Mohammed, Miriam Reshotko, Frank Robertson, Scott List, Ian Young, Kenneth Cadien, "On-Chip Optical Interconnects", *Intel Technology Journal*, **Vol. 8**, Issue 2, pp. 129-141, 2004.

[2] Tetsuo Horimatsu, TakeoIwama, Youichi Oikawa, Takashi Touge, Masao Makiuchi, Osamu Wada, TakakiyoNakagam, "Compact Transmitter and Receiver Modules with Optoelectronic-Integrated Circuits for Optical LAN's", *Journal of Lightwave Technology*, **Vol.4**, No.6, pp.680-688, 1986.

[3] Osama Wada, "Advances in Optoelectronic Integration", *International Journal of High Speed Electronics and Systems,* **Vol. 01**, Issue 01, pp. 47-71, 1990.

[4] http://www.rp-photonics.com/semiconductor_lasers

[5] Kanbara Nobuhiko, Noda Ryuuitirou, Yano Tetsuo, Saito Hiroki , Fujimura Naoyuki, Nishiyama Nobuhiko, "High Speed Micromechanically Tunable Surface Emitting Laser With Si-Mems Technology",*Photonics Technology*, No.47, pp. 45- 48, 2009.

[6] Chunmeng Wu, Toshihiko Makino, S. Iraj Najafi, Romain Maciejko, Mikelis Svilans, Jan Glinski, Mahmoud Fallahi, "Threshold Gain and Threshold Current Analysis of Circular Grating DFB and DBR Lasers", *IEEE Journal Of Quantum Electronics*, **Vol. 29**, No. 10, pp. 2596-2606, 1993.

[7] M.S Unlu, M. K. Emsley, O. I. Dosunmu, P. Muller, Y. Leblebici , "High-speed Si resonant cavity enhanced photodetectors and arrays", *J. Vac. Sci. Technol.*, **Vol. 22**, No.3, pp. 781-787, 2003.

[8] Jianfei Wang, Juejun Hu, Piotr Becla, Anuradha M. Agarwal, Lionel C. Kimerling, "Resonant-cavity-enhanced mid-infrared photodetector on a silicon platform", *Optics Express,* **Vol. 18**, No. 12, pp. 12890-12896, 2010.

[9] G. Cocorullo, M. Iodice, and I. Rendina, "All-silicon Fabry–Perot modulator based on the thermo-optic effect", *Opt. Lett.*, **Vol. 19**, No. 6, pp. 420–422, 1994.

[10] PhotodeteS. C. Strite, and M. S. unlu, "Tunable Photodetectors and Light Emitting Diodes for Wavelength Division Multiplexing", *Electronics Letters*, **Vol. 31**, No. 8, pp. 672-674, 1995.

[11] Zanyun Zhang, Beiju Huang, Zan Zhang, Chuantong Chen, Hongda Chen, "Bidirectional grating coupler based optical modulator for low-loss Integration and low-cost fiber packaging", *Optics Express*, **Vol. 21**, pp. 14202- 14214, 2013.

[12] Thermo opt G. Cocorullo, M. Iodice, and I. Rendina, "All-silicon Fabry–Perot modulator based on the thermo-optic effect", *Opt. Lett.*, **Vol. 19**, No. 6, pp. 420-422, 1994.

[13] G.V. Treyz, P. G. May, and J.M. Halbout, "Silicon Mach–Zehnder waveguide interferometers based on the plasma dispersion effect", *Appl. Phys Lett.*, **Vol. 59**, No. 7, pp. 771-773, 1991.

[14] Connie J. Chang-Hasnain and Weijian Yang, "High-contrast gratings for integrated optoelectronics", *Advances in Optics and Photonics*, **Vol. 4**, pp. 379-440, 2012.

[15] Holographic Transmission Gratings for Spectral Dispersion, LLE Review **Vol. 82**, pp.71-77.

[16] Hongqiang Li, Wenqian Zhou, Yu Liu, Xiaye Dong, Cheng Zhang, Changyun Miao, Meiling Zhang, Enbang Li, Chunxiao Tang, "Preliminary Investigation of an SOI-based Arrayed Waveguide Grating Demodulation Integration Microsystem", *Scientific Reports*, pp.1-6, 2013.

[17] Li PEI , Tigang NING, Fengping YAN, Xiaowei DONG, Zhongwei TAN, Yan LIU, Shuisheng JIAN, "Dispersion compensation of fiber Bragg gratings in 3100 km high speed optical fiber transmission system", *Front. Optoelectron. China*, **Vol. 2**, No.2, pp. 163-169, 2009.

[18] Andrea Irace and Giovanni Breglio, "Silicon-based optoelectronic filters based on a Bragg grating and P-i-N diode for DWDM optical networks", *Proceedings of SPIE*, **Vol. 4947**, pp 68-73, 2003.

[19] M.G. Moharam, T.K. Gaylord, "Rigorous Coupled Wave Analysis of planar-grating diffraction", *J. Opt. Soc. Amer. B*, **Vol. 71**, No. 7, pp.811-818, 1981.

[20] D. Rittenhouse, "Explanation of an optical deception", *Trans. Amer. Phil. Soc*., **Vol. 2**, pp. 37-42, 1786.

[21] Torkel D. Engeness, Mihai Ibanescu, Steven G. Johnson, Ori Weisberg, Maksim Skorobogatiy, Steven Jacobs, and Yoel Fink, "Dispersion tailoring and compensation by modal interactions in OmniGuide fibers", *Optics Express*, **Vol. 11**, Issue 10, pp. 1175-1196, 2003.

[22] T. Miura, F. Koyama, Y. Aoki, A. Matsutani, K. Iga, "Hollow Optical Waveguide for Temperature-Insensitive Photonic Integrated Circuits", *Japanese Journal of Applied Physics*, **Vol. 40**, 2001, L688.

[23] Mukesh Kumar, "Polarization insensitive hollow optical waveguide", *Optics Communications*, **Vol. 285**, pp. 2360-2362, 2012.

[24] Mukesh Kumar, Chris Chase, Vadim Karagodsky, Takahiro Sakaguchi, Fumio Koyama, Connie J. Chang-Hasnain, "Low Birefringence and 2-D Optical Confinement of Hollow Waveguide With Distributed Bragg Reflector and High-Index-Contrast Grating", *IEEE Photonics Journal*, **Vol. 1**, No. 2, pp. 135-143, 2009.

[25] W. Bogaerts, R. Baets, P. Dumon, V. Wiaux, S. Beckx, D. Taillaert, B. Luyssaert, J.Van Campenhout, P. Bienstman, D. Van Thourhout, "Nanophotonic waveguides in silicon-on-insulator fabricated with CMOS technology", *J. Lightwave Technol*., **Vol. 23**, pp. 401-412, 2005.

[26] R.M. Emmons, D.G. Hall, "Buried-oxide silicon-on-insulator structures wave-guide grating couplers", *IEEE J. Quant. Electron*., **Vol. 28**, pp. 164-175,1992.

[27] T. Suhara, H. Nishihara, "Integrated-optics components and devices using periodic structures", *IEEE J. Quant. Electron.*, **Vol. 22**, Issue 6, pp. 845-867, 1986.

[28] Y. Zhou, M. Moewe, J. Kern, M. C. Y. Huang, and C. J. Chang-Hasnain, "Surface-normal emission of a high-Q resonator using a subwavelength high-contrast grating", *Opt. Exp.*, **Vol. 16**, pp. 17282-17287, 2008.

[29] Y. Zhou, V. Karagodsky, B. Pesala, F. G. Sedgwick, and C. J. Chang- Hasnain, "A novel ultra-low loss hollow-core waveguide using subwavelength high-contrast gratings," *Opt. Exp.*, **Vol. 17**, pp. 1508-1517, 2009.

[30] Michael C.Y. Huang, Y. Zhou And Connie J. Chang-Hasnain, "A surface-emitting laser incorporating a high-index-contrast subwavelength grating", *Nature Photonics*,**Vol.1**, pp. 119-122**,** 2007.

[31] Ye Zhou, Michael C.Y.Huang, Connie J. Chang-Hasnain, "Tunable VCSEL with ultra-thin high contrast grating for high-speed tuning", *Optics Express*, **Vol. 16**, pp. 14221-14226, 2008.

[32] Christopher Chase, Ye Zhou, Connie J. Hasnain, "Size effect of high contrast gratings in VCSELs", *Optics Express*, **Vol. 17,** pp. 24002-24007, 2009.

[33] Christopher Chase, Yi Rao, Werner Hofmann, Connie-Hasnain, "1550 nm High contrast grating VCSEL", *Optics Letters*, **Vol. 18**, pp.15461-15466, 2010.

[34] Connie J. Chang-Hasnain ,Ye Zhou, Michael C.Y. Huang, Christopher Chase, "High-Contrast Grating VCSEL", *IEEE Journal Of Selected Topics In Quantum Electronics*, **Vol. 15**, No. 3, pp. 869-877, 2009.

[35] Werner Hofmann, ChrisChase, ConnieJ.Chang-Hasnain, Gerhard, "Long-Wavelength High-Contrast Grating Vertical-Cavity Surface-Emitting Laser", *IEEE Photonics Journals*, **Vol.2**, No.3, pp. 415-422, 2010.

[36] Ye Zhou, Michael C.Y. Huang, Connie J. Chang- Hasnain,"Large Fabrication Tolerance for VCSELs using high contrast grating", *IEEE Photonics Technology Letters*,**Vol.20**, No.6, pp. 434-436, 2008.

[37] Ye Zhou, Michael C.Y.Huang, Christopher Chase, Vadim Karagodsky, "High-Index-Contrast Grating (HCG) and Its Applications in Optoelectronic Devices", *IEEE Journal of Selected Topics In Quantum Electronics*, pp. 1077-260X, 2009.

[38] Connie J Chang-Hasnain, "High-contrast gratings as a new platform for integrated optoelectronics", *Semicond. Sci. Technol*., **Vol. 26**, pp.1-12, 2011.

[39] D. Fattal, J. J. Li, Z. Peng, M. Fiorentino, R. G. Beausoleil, "Flat dielectric grating reflectors with focusing abilities", *Nat. Photonics*, **Vol. 4**, pp. 466-470, 2010.

[40] J. Niehusmann, A. Vörckel, P. H. Bolivar, T. Wahlbrink, W. Henschel, H. Kurz, "Ultrahigh-quality-factor silicon-on-insulator microring resonator", *Opt. Lett*., **Vol. 29**, pp. 2861-2863, 2004.

[41] B. Jalali, S. Yegna narayanan, T. Yoon, T. Yoshimoto, I. Rendina, F. Coppinger, "Advances in Silicon-on-Insulator Optoelectronics", *IEEE Journal of Selected Topics In Quantum Electronics*, **Vol. 4**, No. 6, pp. 938 – 947, 1998

[42] Richard A. Soref, "Silicon-Based Optoelectronics", *Proceedings of the IEEE*, **Vol. 81**, No. 12, pp. 1687-1706, 1993.

[43] B. G. Lee, X. Chen, A. Biberman, X. Liu, I.-W. Hsieh, C.-Y. Chou, J. I. Dadap, F. Xia, W. M. J. Green, L. Sekaric,Y. A. Vlasov, R.M. Osgood, Jr., K. Bergman, "Ultrahigh-bandwidth silicon

photonic nanowire waveguides for on-chip networks", *IEEE Photon. Technol. Lett.*, **Vol. 20**, No. 6, pp. 398–400, 2008.

[44] Yong Zhang, Mei Han and Cheng-Ping Huang, "Enhanced absorption and optical force in a sandwiched grating at the terahertz band", EPL, 102, pp. 34001-1-5, 2013.

[45] Mingbo Pu, Min Wang, Chenggang Hu, Cheng Huang, Zeyu Zhao, Yanqin Wang, Xiangang Luo, "Engineering heavily doped silicon for broadband absorber in the terahertz regime", *Optics Express*, **Vol. 20,** pp. 25513-25519, 2012.

[46] Hou-Tong Chen, Richard D. Averitt, Willie J. Padilla, Joshua M. O. Zide, Arthur C. Gossar, Antoinette J. Taylor, "Active terahertz metamaterial devices", *Nature*, **Vol. 444**, pp. 597-600, 2006.

[47] Hu Tao, C. M. Bingham, A. C. Strikwerda, D. Pilon, W. J. Padilla, D. Shrekenhamer, R. D. Averitt, N. I. Landy, K. Fan, X. Zhang, "Highly flexible wide angle of incidence terahertz metamaterial absorber: Design, fabrication, and characterization", *Physical Review* B, **Vol. 78**, pp. 241103-1-4, 2008.

[48] Owen P. Marshall, Md. Khairuzzaman, Harvey E. Beere, David A. Ritchie, Subhasish Chakraborty, "Broadband photonic control for dual-mode terahertz laser emission", *Applied Physics Letters,* **Vol. 102**, pp. 181106-1-4, 2013.

[49] N. I. Landy, S. Sajuyigbe, J. J. Mock, D. R. Smith, W. J. Padilla1, "Perfect Metamaterial Absorber", *Physics Review Letters,* **Vol.100**, pp. 207402-1-6, 2008.

[50] J. J. Greffet, R. Carminati, K. Joulain, J. P. Mulet, S. P. Mainguy, Y. Chen, "Coherent emission of light by thermal sources", *Nature,* **Vol. 416**, pp. 61–64, 2002.

[51] M. Diem, T. Koschny, C. M. Soukoulis, "Wide-angle perfect absorber/thermal emitter in the terahertz regime", *Phys. Rev. B,* **Vol. 79**, No.3, pp. 033101-1-4, 2009.

[52] Peter Bienstman, Peter Vandersteegen, Roel Baets, "Modelling gratings on either side of the substrate for light extraction in light-emitting diodes", *Optical and Quantum Electronics,* **Vol. 39**, pp. 797-804, 2007.

[53] C. Cheng, A. Scherer, R.C. Tyan, Y. Fainman, G. Witzgall, E. Yablonovitch,"New fabrication techniques for high quality photonic crystal", *J. Vac. Sci. Technol. B,* **Vol. 15**, pp. 2764-2767; doi: 10.1116/1.589723, 1997.

[54] Carlos F. R. Mateus, , Michael C. Y. Huang, Lu Chen, Connie J. Chang-Hasnain,Yuri Suzuki, "Broad-Band Mirror Using a Subwavelength Grating", *IEEE photonics technology letters*, **Vol. 16**, No. 7, pp. 1676-1678, 2004.

[55] C. F. R. Mateus, M. C. Y. Huang, D. Yunfei, A. R. Neureuther, C. J. Chang-Hasnain, "Ultrabroadband mirror using low-index cladded subwavelength grating", *IEEE Photon. Technology Letters,* **Vol. 16**, No. 2, pp. 518–520, 2004.

[56] H. A. Haus, Y. Lai, "Narrow-band distributed feedback reflector design", *J. Lightwave Technol*., **Vol. 9**, pp. 754-760, 1991.

[57] Olivier Parriaux, Thomas Kämpfe, FrédéricGaret, Jean-Louis Coutaz, "Narrow band, large angular width resonant reflection from a periodic high index grid at terahertz frequency", *Optics Express*, **Vol. 20**, pp. 28070-28081**,** 2012.

[58] N. Destouches, J.C. Pommier, and O. Parriaux, "Narrow band resonant grating of 100%reflection under normal incidence", *Optics Express*, **Vol. 14**, pp. 12613-12622**,** 2006.

[59] Ye Zhou, Michael C.Y. Huang Connie J. Chang-Hasnain, "Transverse Mode Control in High-Contrast Subwavelength Grating VCSEL", CTuX1, 2007.

[60] Junichi Kashino, Shunya Inoue, Akihiro Matsutani, Hideo Ohtsuki, Takahiro Miyashita, Fumio Koyama "Transverse Mode Control of VCSELs Using Angular Dependent High-contrast Grating Mirror", *IEEE TUE*2.2, pp. 244-245, 2013.

[61] Michael C.Y. Huang, and Connie J. Chang-Hasnain, "Polarization Mode Control in High Contrast Subwavelength Grating VCSEL", *IEEE Conference On Laser And Electrooptics(CLEO)2008.*

[62] Vadim Karagodsky, Bala Pesala, Christopher Chase, Werner Hofmann, Fumio Koyama Connie J.Chang-Hasnain, "Monolithically integrated multi-wavelength VCSEL arrays using high-contrast gratings", *Optics Express*, **Vol. 18**, pp. 694-699, 2010.

[63] J. M. Foley, S. M. Young, J. D. Phillips, "Narrowband mid-infrared transmission filtering of a single layer dielectric grating", *Applied Physics Letters*, **Vol. 103**, pp. 071107-1-5, 2013.

[64] Ben-Xin Wang, Ling-Ling Wang, Gui-Zhen Wang, Wei-Qing Huang, Xiao-Fei Li, Xiang Zhai, "Theoretical Investigation of Broadband and Wide-Angle Terahertz Metamaterial Absorber", *IEEE Photonics Technology Letters*, **Vol. 26**, No. 2, pp. 111-114, 2014.

[65] Mukesh Kumar, "Narrow bandwidth and polarization independent design of hollow waveguide in-plane mirror with ultra-wide tuning range", *Applied Optics*, **Vol. 52**, Issue 9, pp.1847-1851, 2013.

[66] Fumio Koyama, "Engineering of angular dependence of high-contrast grating mirror for transverse mode control of VCSELs", *Proc. SPIE* 8995, High Contrast Metastructures III, 89950H (2014); doi:10.1117/12.2042069